Mineralogical Magazine

The occurrence of the REE-vanadate wakefieldite in the rhyolitic Joe Lott Tuff

--Manuscript Draft--

Manuscript Number:	
Full Title:	The occurrence of the REE-vanadate wakefieldite in the rhyolitic Joe Lott Tuff
Short Title:	Wakefieldite in rhyolitic tuff
Article Type:	Article
Section/Category:	General submission
Keywords:	Joe Lott Tuff; wakefieldite-(Nd); wakefieldite-(Y); As, P and Th enrichment.
Corresponding Author:	Bogus?aw Bagi?ski University of Warsaw, Institute of Geochemistry, Mineralogy & Petrology, Faculty of Geology mazowieckie, POLAND
Corresponding Author Secondary Information:	
Corresponding Author's Institution:	University of Warsaw, Institute of Geochemistry, Mineralogy & Petrology, Faculty of Geology
Corresponding Author's Secondary Institution:	
First Author:	Bogus?aw Bagi?ski
First Author Secondary Information:	
Order of Authors:	Bogus?aw Bagi?ski
	Ray Macdonald, prof
	Harvey E. Belkin, dr
	Jakub Kotowski
	Petras Jokubauskas, dr
	Beata Marciniak-Maliszewska, dr
Order of Authors Secondary Information:	
Manuscript Region of Origin:	POLAND
Abstract:	The high-silica rhyolitic Joe Lott Tuff was erupted at 19.2 ± 0.4 Ma from the Mount Belknap caldera, SW Utah. Certain units in the tuff contain two species of wakefieldite, the Nd- and Y-dominant types. They occur in disseminated streaks and patches in association with rhodochrosite, calcite, Fe oxide, cerite, and a Mn silicate (caryopilite?), thought to have been deposited from hydrothermal fluids. The wakefieldites contain the highest levels of As (≤15.34 wt.% As2O5) and P (≤5.7 wt.% P2O5) yet recorded in the mineral, pointing to significant solid solution towards chernovite and xenotime. Thorium levels are also unusually high (≤14.2 wt.%). The source of the hydrothermal fluid(s) is unknown but may be related to uranium mineralization in the region, in that As, V and U are commonly associated in such deposits.
Suggested Reviewers:	Adam Pieczka, dr professor, Akademia Gorniczo-Hutnicza imienia Stanislawa Staszica w Krakowie Wydzial Geologii Geofizyki i Ochrony Srodowiska pieczka@agh.edu.pl expertise in accessory minerals
	Dmitry Zozulya, dr research scientist, Institut geologii i mineralogii imeni V S Soboleva SO RAN zozulya@geoksc.apatity.ru expertise in mineralized igneous rocks

	Igor Broska, dr Geological Survey of Slovakia igor.broska@savba.sk expertise in accessory minerals
Opposed Reviewers:	
Additional Information:	
Question	**Response**
I have re-examined my references and determined that I have cited all relevant articles published within the past 24 months (including those in Mineralogical Magazine).	Yes

The occurrence of the REE-vanadate wakefieldite in the rhyolitic Joe Lott Tuff, Utah, USA

B. BAGIŃSKI[1*], R. MACDONALD[1,2], H. E. BELKIN[3], J. KOTOWSKI[1], P. JOKUBAUSKAS[1] AND B. MARCINIAK-MALISZEWSKA[1]

[1] Institute of Geochemistry, Mineralogy and Petrology, University of Warsaw, 02-089 Warsaw Poland

[2] Environment Centre, Lancaster University, Lancaster LA1 4YQ, UK

[3] U.S. Geological Survey, retired, 11142 Forest Edge Drive, Reston, VA 20190-4026, USA

*Corresponding author: e-mail: B.Baginski1@uw.edu.pl

Running head: Wakefieldite in rhyolitic ignimbrite

ABSTRACT

The high-silica rhyolitic Joe Lott Tuff was erupted at 19.2 ± 0.4 Ma from the Mount Belknap caldera, SW Utah. Certain units in the tuff contain two species of wakefieldite, the Nd- and Y-dominant types. They occur in disseminated streaks and patches in association with rhodochrosite, calcite, Fe oxide, cerite, and a Mn silicate (caryopilite?), thought to have been deposited from hydrothermal fluids. The wakefieldites contain the highest levels of As (≤15.34 wt.% As_2O_5) and P (≤5.7 wt.% P_2O_5) yet recorded in the mineral, pointing to significant solid solution towards chernovite and xenotime. Thorium levels are also unusually high (≤14.2 wt.%). The source of the hydrothermal fluid(s) is unknown but may be related to uranium mineralization in the region, in that As, V and U are commonly associated in such deposits.

KEYWORDS: Joe Lott Tuff, wakefieldite-(Nd), wakefieldite-(Y), As, P and Th enrichment.

Introduction

Four species of the *REE*-vanadate wakefieldite are known: wakefieldite-(Ce) (Deliens and Piret, 1977, 1986), wakefieldite-(La) (Witzke *et al*., 2008), wakefieldite-(Nd) (Moriyami *et al*., 2010), and wakefieldite-(Y) (Miles *et al*., 1971). They occur in a large number of parageneses, including Fe-Mn deposits, granitic pegmatites and silicified wood, and in a wide range of mineral associations. All occurrences of which we are aware, and their host rocks, are listed in the Supplementary Material. The total number is 23, although some reports are not accompanied by confirmatory X-ray diffraction or electron microprobe analytical data. Published analyses have shown that there is considerable compositional variation in wakefieldite, with significant degrees of solid solution between each species and with chernovite ($YAsO_4$) and xenotime (YPO_4). Calcium, Si and Th can also be significant components.

This paper describes previously unrecorded wakefieldite-(Nd) and wakefieldite-(Y) from a high-silica rhyolitic ash-flow deposit, the Joe Lott Tuff, Utah, USA. The new data have allowed us to comment on compositional variation in the phase and to propose the major substitution schemes. It is suggested that the wakefieldite crystallized from carbonate-rich fluids possibly associated with local vanadium-uranium mineralization.

Joe Lott Tuff

The Joe Lott Tuff Member of the Mount Belknap Volcanics is a rhyolitic ash flow tuff sheet associated with the collapse of the Mount Belknap caldera in west-central Utah (Fig. 1; Cunningham and Steven, 1979; Budding *et al*., 1987). Erupted at 19.2 ± 0.4 Ma, it has a

volume of 150 km^3. The tuff is a composite sheet, changing laterally from a single cooling unit near source to four distinct cooling units distally (Fig. 2). The Lower Unit is up to 64 m thick and has a basal vitrophyre. Initial collapse of the caldera accompanied eruption of the Lower Unit. The unit is followed upward by a Middle Unit up to 43 m thick, a 26 m thick Pink Unit, and an Upper Unit 31 m thick. The poorly welded, pumice-rich Pink Unit comprises two ash-flow tuffs (17 m and 9 m thick) separated by a fall layer 0.5 m thick (Fig. 3).

The major variability in the tuff is in the degree of welding and the abundance of phenocryst phases. The most densely welded, eutaxitic, rocks are at the base of the Lower Unit (the basal vitrophyre); the degree of welding increases upwards in both the Lower and Middle Units (Budding *et al*., 1987). With the exception of the basal vitrophyre, the groundmass of all samples is largely devitrified.

Occurrence of wakefieldite

Wakefieldite has been studied in two samples; M831, from the upper part of the Middle Unit, and JLT4.1, from the upper ash-flow layer in the Pink Unit. M831 is poorly welded, with pumices and shards in a devitrified matrix rich in lithophysae up to 0.7 mm across. It contains about 1 modal % phenocrysts of quartz, sanidine, plagioclase, augite, FeTi oxides, apatite, zircon and monazite (Budding *et al*., 1987). JLT4.1 is more densely welded and lithophysae-bearing, with the main phenocrysts being alkali feldspar, quartz and magnetite.

The wakefieldite occurs in disseminated veins and patches, associated with rhodochrosite, calcite, Fe oxides, cerite, a Mn silicate (caryopilite?), monazite and quartz (Fig. 4). The assemblage is similar to that of the type wakefieldite-(Nd) from the Arose stratiform deposit,

Japan, reported by Moriyama *et al.* (2010) as hematite, caryopilite, calcite and rhodochrosite. In the Joe Lott tuff, the wakefieldite is relatively abundant: in JLT4.1, over 100 crystals have been identified in a single thin section. Crystals are invariably small; the majority are ≤5 μm across, although a few are up to 10 μm. Representative occurrences of wakefieldite-(Nd) are shown in Fig. 5, in two cases being associated with rhodochrosite and in two associated with magnetite phenocrysts. The crystals show several forms, including platy, prismatic and rounded. Contacts with neighbouring minerals are normally very sharp.

Analytical methods

Accessory phases were initially identified by SEM, using a Zeiss Σigma^{TM}/VP FE (field emission) – SEM equipped with new generation SDD-type two EDS (XFlash 6/10^{TM}) detectors produced by Bruker. An acceleration voltage of 30 kV and a 120 μm aperture were used. Mineral compositions were determined by electron microprobe, using a Cameca Five FE microprobe equipped with five wavelength dispersive spectrometers and large crystals. The analytical conditions were: accelerating voltage 15 kV and probe current 40 nA, with counting times of 20 s on peak and 10 s on each of two background positions. The standards, crystals and X-ray lines used, and approximate detection limits are given in Table 1. The 'PAP'φ(ρZ) program of Pouchou and Pichoir (1991) was used for corrections.

Mineral compositions

Composition of wakefieldite-(Nd) and wakefieldite-(Y)

Sample JLT4.1 contains both wakefieldite-(Nd) and wakefieldite-(Y); M831 has only wakefieldite-(Y) (Fig. 6; Table 1). After Nd, the most abundant *REE* in wakefieldite-(Nd) is La, followed by Y. Total *REE*+Y are in the range 0.82-0.90 apfu. The chondrite-normalized *REE* patterns (Fig. 7a) show strong negative Ce anomalies (Ce/Ce* 0.08-0.18), peaks at Pr, then a steady decrease to the *HREE* with large negative Eu anomalies (Eu/Eu* 0.06-0.30). The minor troughs at Ho in some patterns may be an artefact since the levels of the element are close to the detection limits. Inter-crystal variations are exemplified by $[La/Ce]_{CN}$ (4-12) and $[La/Yb]_{CN}$ (6-24). The dominant cations replacing the *REE* are Ca (≤0.05 apfu) and Th (0.05-0.09 apfu). Arsenic (0.03-0.11 apfu) is the main substituent for V (0.77-0.89 apfu), with lesser amounts of P (0.02-0.04 apfu) and Si (≤0.04 apfu).

Compared to the Nd-dominant variety, wakefieldite-(Y) in M831 has higher Th (0.05-0.15 apfu), As (0.05-0.37 apfu), P (0.04-0.11 apfu) and Si (≤0.20 apfu), and lower *REE*+Y (0.69-0.75 apfu), and V (0.36-0.76 apfu). The crystals show, with one exception, positive Ce anomalies (Ce/Ce* 1.4-2.2), peak at Sm and have negative Eu anomalies (Eu/Eu* 0.13-0.26) (Fig. 7b). The wakefieldite-(Y) contains ≤0.18 wt% SO_3 (≤0.01 apfu). The only other report of anions in wakefieldite of which we are aware is of SO_3 in fossilized wood from the Czech Republic (0.14 wt.%; Matysova *et al*., 2016), although Khoury *et al*. (2015) refer to the occurrence in marbles in central Jordan of a Ca-rich, U-and S-bearing analogue of wakefieldite-(Ce) [$(Ce,Ca,U)(VO_4)(SO_4)$]. The wakefieldite-(Y) from sample JLT4.1 is different to that in sample M831 in having lower abundances of As, P, Th and V (Fig. 8). The patterns in chondrite-normalized *REE* plots in JLT4.1 are broadly similar to those for wakefieldite-(Nd) in the same rock (Figs. 7a, 7b).

Substitution mechanisms

In this section, the new and published analyses are used to look for generally applicable substitution schemes. Among the *REE*, the main substitutions are Y_1HREE_{-1} (Fig. 9a) and $LREE_1(Y, HREE)_{-1}$ (Fig. 9b). Calcium may be incorporated into wakefieldite by the substitution $Ca^{2+} + Th^{4+} = 2(REE+Y)^{3+}$, as is observed in *inter alia* the monazite group but the overall correlation is not strong (Fig.10a; $r^2 = 0.32$) because the various suites follow separate subtrends.

The major substituent for V in the Joe Lott samples is As (As_1V_{-1}), with As levels up to 0.37 apfu (15.34 wt.% As_2O_5) in wakefieldite-(Y) (Fig. 8a). These are the highest values yet recorded in wakefieldite. In their study of *LREE*- and Y-arsenates from a Fe-Mn deposit in the Maritime Alps, Miyawaki and Nakai (1996) found up to 30 mol% of $LREEVO_4$, broadly similar in amount to the entry of As into wakefieldite. Phosphorus also substitutes for V (P_1V_{-1}) in significant amounts in the Joe Lott minerals (≤0.11 apfu; 5.7 wt.% P_2O_5), again the highest values yet recorded in wakefieldite (Fig.8b). It is still uncertain, however, whether there is a complete $YVO_4 – YPO_4$ solid solution (Kolitsch and Holtstam, 2004; Hetherington *et al*., 2008). Silicon is present at levels ≤0.19 apfu (4.1 wt.% SiO_2), although some high values may be due to beam contamination by neighbouring quartz grains. The mechanism of incorporation of Si is uncertain: one possibility is similar to the thorite exchange in xenotime, $Y^{3+} + P^{5+} = Th^{4+} + Si^{4+}$ (Förster, 2006), as inferred by Miles *et al*. (1971) for the type wakefieldite-(Y); however, the correlation in the Joe Lott tuff data is weak ($r^2 = 0.34$) (Fig. 10b).

As noted above, in their study of *LREE*- and Y-arsenates Miyawaki and Nakai (1996) found up to 30 mol.% of $LREEVO_4$, in LREE- and Y-arsenates. They suggested that the presence of large AsO_4 tetrahedra could enable Y-arsenates to accept the larger *LREE* ions. In

140 the Joe Lott case, however, the situation is reversed: the highest As contents are accompanied
141 by higher *HREE*+Y and lower *LREE* (Figs. 11a, b).

142

143 **Formation conditions**

144 The wakefieldite-(Nd) and wakefieldite-(Y) in the Joe Lott Tuff are found in veins and
145 patches associated with rhodochrosite, calcite, cerite, monazite, quartz, Fe-oxide and
146 caryopilite (?), strongly suggesting that they are of hydrothermal origin. This is consistent
147 with the negative Ce anomalies in wakefieldite-(Nd): the mineral was formed in fluids
148 depleted in Ce by oxidation of Ce^{3+}, with the Ce then entering cerite (c.f. Witzke *et al*., 2008).
149 We have no independent evidence of the T-P conditions under which they crystallized.
150 However, Bakker and Elburg (2006) found that wakefieldite- (Ce) in diopside-titanite veins in
151 Arkaroola, Flinders Range, South Australia, was formed by remobilization of *LREE* and Y
152 from titanite and/or the granitic host rock by a hydrothermal fluids of fairly pure H_2O at T
153 $<200^0$C and P <50 MPa.

154 The large number of parageneses in which wakefieldite has been found is reflected in the
155 many mechanisms proposed for its formation. Miles *et al.* (1971) proposed that the type
156 wakefieldite-(Y) is a secondary mineral, possibly derived by leaching of Y-bearing hellandite
157 [$(Ca,REE)_4Y_2Al_2(Si_4B_4O_{22})(OH_2)$]. The type wakefieldite-(Ce) was formed, along with
158 vanadinite [$Pb_5(VO_4)_3Cl$], in an oxidation zone in a silicified limestone (Deliens and Piret,
159 1977). Howard *et al*. (1995) reported wakefieldite-(Ce) occurring with Sr-rich zeolites and
160 fluorite, suggesting that the *REE* and V were carried by hydrothermal solutions during the last
161 stages of formation of the zeolites. Wakefieldite-(Ce) occurs with roscoelite, a vanadium
162 mica, in reduction spots in Devonian sandstones in Banffshire, Scotland. The roscoelite is

thought to have formed by a reaction involving a change in redox potential of the groundwater and the release of V from V-rich Fe-Ti oxides in the sandstone (van Panhuys-Sigler *et al*., 1996). Moriyami *et al*. (2010) proposed that the type wakefieldite-(Nd) was formed during prehnite-pumpellyite facies metamorphism by recrystallization and hydration of Fe-and Mn-hydroxide. A solid solution of wakefieldite-(Ce) and wakefieldite-(Y) was formed in silicified plant issue of Lower Palaeozoic age from the Studenec area, Czech Republic, as a secondary mineral during post-depositional diagenesis (Matysova *et al*., 2016).

The association of wakefieldite with carbonates in the Joe Lott Tuff strongly suggests that the mineral was deposited from CO_2-rich hydrothermal fluids but this study has provided no evidence of the source of the inferred fluids. However, the Mount Belknap Volcanics (23-14 Ma) formed above a western and eastern source area spanning the central part of the Marysvale volcanic field (Fig. 1). Intrusions in the source area resulted in hydrothermally altered rocks and deposits mostly of uranium and molybdenum (Rowley *et al*., 1994). The uranium mines in the Marysvale region were operated by the Vanadium Corporation of America. While the mineralization described in this paper is clearly of a different type, it may also have been related to fluids released by these intrusions.

Acknowledgements

We thank Dr Uwe Kolitsch for kindly supplying us with a copy of the 2011 paper by Gröbner *et al.* on the Harz Mountains occurrence (see Supplementary Material). The work was supported through the Innovative Economy Operational Program POIG.02.02.00-00-025/09 (NanoFun; Cryo-SEM microscopy lab). Financial support was also provided by the project BSt 185704 IGMiP.

References

Bakker, R.J. and Elburg, M.A. (2006) A magmatic-hydrothermal transition in Arkarooola (northern Flinders Ranges, South Australia): from diopside-titanite pegmatites to hematite-quartz growth. *Contributions to Mineralogy and Petrology*, **152**, 541-569.

Baudracco-Gritti, C., Quartieri, S., Vezzalini, G., Permingeat, F., Pillard, F. and Rinaldi, R. (1987) Une wakefieldite-(Ce) non plombifère: nouvelles données sur l'espèce minérale correspondant à l'orthovanadate de cérium. *Bulletin Minéralogique*, **110**, 657-663.

Budding, K.E., Cunningham, C.G., Zielinski, R.A., Steven, T.A. and Stern, C.R. (1987) Petrology and chemistry of the Joe Lott Tuff Member of the Mount Belknap Volcanics, Marysvale volcanic field, west-central Utah. *U.S. Geological Survey Professional Paper*, **2354**, 47 pp.

Cunningham, C.G. and Steven, T.A. (1979) Mount Belknap and Red Hills calderas and associated rocks, Marysvale volcanic field, west-central Utah. *U.S. Geological Survey Bulletin*, **1468**, 34 p.

Deliens, M. and Piret, P. (1977) La kusuïte (Ce^{3+}, Pb^{2+}, Pb^{4+})VO_4, nouveau minéral. *Bulletin de la Société Française de Minéralogie et Cristallographie*, **100**, 39-41.

Deliens, M. and Piret, P. (1986) La kusuïte devient la wakefieldite-(Ce) plombifère. *Bulletin de Minéralogie*, **109**, 305.

Förster, H.-J. (2006) Composition and origin of intermediate solid solutions in the system

thorite-xenotime-zircon-coffinite. *Lithos*, **88**, 35-55.

Hetherington, C.J., Jercinovic, M.J., Williams, M.L. and Mahan, K. (2008) Understanding geologic processes with xenotime: Composition, chronology, and a protocol for electron probe microanalysis. *Chemical Geol*ogy, **254**, 133-147.

Howard, D.G., Tschernich, R.W. and Klein, G.L. (1995) Occurrence of wakefieldite-(Ce) with zeolites at Yellow Lake, British Columbia, Canada. *Neues Jahrbuch für Mineralogie Monatshefte*, **3**, 127–132.

Khoury, H.N., Sokol, E.V. and Clark, I.D. (2015) Calcium uranium oxide minerals from central Jordan: assemblages, chemistry, and alteration products. *The Canadian Mineralogist*, **53**, 61-82.

Kolitsch, U. and Holtstam, D. (2004) Crystal chemistry of $REEXO_4$ compounds (X = P, As, V). II. Review of $REEXO_4$ compounds and their stability fields. *European Journal of Mineral*ogy, **16**, 117-128.

Matysova, P., Götze, J., Leichmann, J., Škoda, R., Strnad, L., Drahota, P. and Grygar, T. (2016) Cathodoluminescence and LA-ICP-MS chemistry of silicified wood enclosing wakefieldite – REEs and V migration during complex diagenetic evolution. *European Journal of Mineralogy*, **28**, 869-887.

Miles, N.M., Hogarth, D.D. and Russell, D.S. (1971) Wakefieldite, yttrium vanadate: a new mineral from Quebec. *American Mineralogist*, **56**, 395-410.

Miyawaki, R. and Nakai, I. (1996) Crystal chemical aspects of rare earth minerals. Pp. 21-40 in: *Rare Earth Minerals. Chemistry, Origin and Ore Deposits* (A.P. Jones, F. Wall and C.T. Williams, editors). Chapman & Hall, London.

228 Moriyami, T., Miyawaki, R., Yokoyama, K., Matsubara, S., Hirano, H., Murukami, H. and
229 Watanabe, Y. (2010) Wakefieldite-(Nd), a new neodymium vanadate mineral in the Arase
230 stratiform ferromanganese deposit, Kochi Prefecture, Japan. *Resource Geology*, **61**, 101-
231 110.
232 Pouchou, J.L. and Pichoir, J.F. (1991) Quantitative analysis of homogeneous or stratified
233 microvolumes applying the model 'PAP'. Pp. 31-75 in: *Electron Probe Quantitation* (H.
234 Newbury, editor). Plenum Press: New York.
235 Rowley, P.D., Mehnert, H.H., Naeser, C.W., Snee, L.W., Cunningham, C.G., Steven, T.A.,
236 Anderson, J.J., Sable, E.G. and Anderson, R.E. (1994) Isotopic ages and stratigraphy of
237 Cenozoic rocks of the Marysvale volcanic field and adjacent areas, west-central Utah. *U.S.*
238 *Geological Survey Bulletin*, **2071**, 35 pp.
239 Sun, S.-S. and McDonough, W.F. (1989) Chemical and isotopic systematics of oceanic
240 basalts: implications for mantle composition and processes. Pp. 313-345 in*: Magmatism in*
241 *the Ocean Basins.* (A.D. Saunders and M.J. Norry, editors). Special Publication of the
242 Geological Society, **42**. Geological Society, London.
243 van Panhuys-Sigler, M., Trewin, N.H. and Still, J. (1996) Roscoelite associated with
244 reduction spots in Devonian red beds, Gamrie Bay, Banffshire. *Scottish Journal of*
245 *Geology*, **32**, 127-132.
246 Witzke, T., Kolitsch, U., Warnsloh, J.M. and Göske, J. (2008) Wakefieldite-(La), $LaVO_4$, a
247 new mineral species from the Glűcksstern Mine, Friedrichroda, Thuringia, Germany.
248 *European Journal of Mineralogy*, **20**, 1135-1139.

Figure captions

Fig. 1. Locality map of the Mount Belknap Caldera in southwestern Utah, USA, showing the distribution of the Joe Lott Tuff and the location of samples (JLT4.1 and M831) used in this study.

Fig. 2. Stratigraphic relationships in the Joe Lott Tuff Member, the underlying Bullion Canyon Volcanics and the overlying crystal-rich member of the Mount Belknap Volcanics (after Budding *et al*., 1987, fig. 4). The approximate positions of samples M831 and JLT4.1 are shown.

Fig. 3. Pink Unit, exposed near the junction of State Road 4 and Interstate 89. Two ash-flows are separated by a thin fall layer (white; arrowed).

Fig. 4. False colour back-scattered electron (BSE) image of a thin section of JLT4.1. The dark cores of the rounded lithophysae (green) are composed of caryopilite (?) and silica. Yellow areas – calcite; red – rhodochrosite, blue – quartz and alkali feldspar. The pink crystal is titanomagnetite.

Fig. 5. BSE images of wakefieldite-(Nd) (Wf). **(a)** In rhodochrosite (Rds) associated with magnetite phenocryst (Mag). **(b)** Associated with magnetite phenocryst, which also has inclusions of cerite (Cer) and ilmenite (Ilm). Afs is an alkali feldspar phenocryst. **(c)** Subhedral crystal embedded in rhodochrosite. Rds is italicised to show the textural difference to that in Fig. 5a; the darker Rds to the right is more calcic. Qtz - quartz. **(d)** As inclusion in magnetite phenocryst. The pale rim marked X is an unidentified Mn, Pb, Al, Ca silicate.

Fig. 6. Ce-Nd-Y (apfu) plot for the Joe Lott Tuff and comparative suites. Data sources: Joe Lott Tuff – Supplementary Table 1; fossilized wood – Matysova *et al.* (2016); Arose – Moriyami *et al*. (2010); Arkaroola – Bakker and Elburg (2006); Tifernine - Baudracco-Gritti *et al*. (1987). Wakefieldite-(La) is not plotted.

Fig. 7. Chondrite-normalized *REE* plots for **(a)** wakefieldite-(Nd) and **(b)** wakefieldite-(Y) in the Joe Lott Tuff. Data source: Supplementary Table 1, analysis numbers 1, 4, 9, 13, 14, 16, 22, 17. Normalizing factors from Sun and McDonough (1989).

Fig. 8. **(a)** V-As and **(b)** V-P plots for Joe Lott Tuff and comparative suites. Data sources as in Figure 6.

Fig. 9. **(a)** Y – *HREE* and **(b)** (Y+*HREE*) – *LREE* plots for Joe Lott Tuff and comparative suites. Data sources as in Fig. 6, plus Glücksstern – Witze *et al*. (2008).

Fig. 10. **(a)** $Ca^{2+} + Th^{4+} = 2(REE + Y)^{3+}$ and **(b)** $Y^{3+} + P^{5+} = Th^{4+} + Si^{4+}$ as possible substitution schemes in wakefieldite.

Fig. 11. Arsenic plotted against **(a)** (*HREE* + Y) and **(b)** *LREE* for Joe Lott Tuff and comparative suites.

Cover letter

The paper reports a very unusual occurrence of the rare mineral wakefieldite in a rhyolitic ignimbrite. New EPMA analyses extend the compositional range of the mineral with especially high values of As and P. The occurrence may have been formed from CO_2 rich metasomatizing fluids.

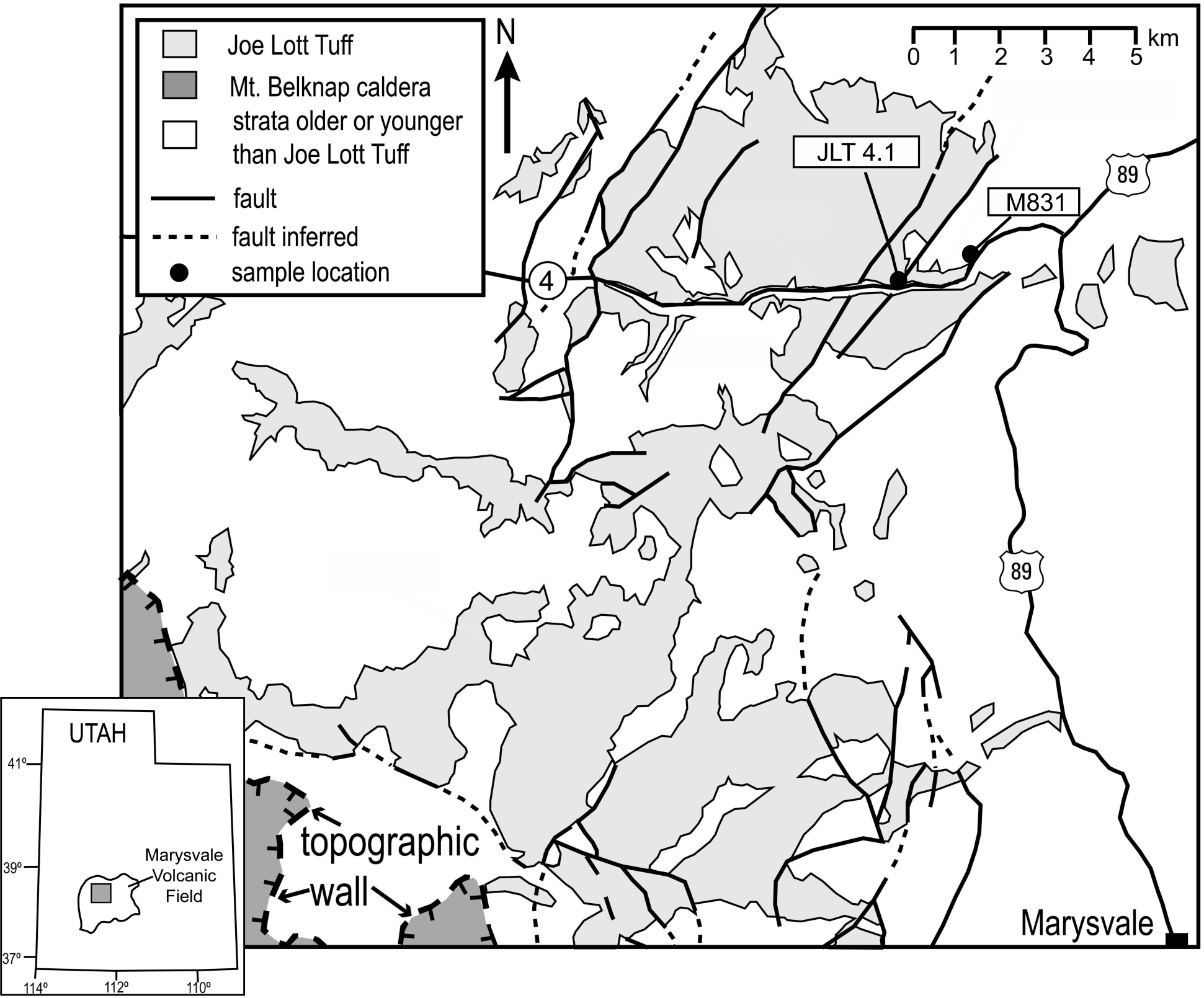

Figure 1

Figure 2

Click here to access/download;Figure;Fig.2.eps

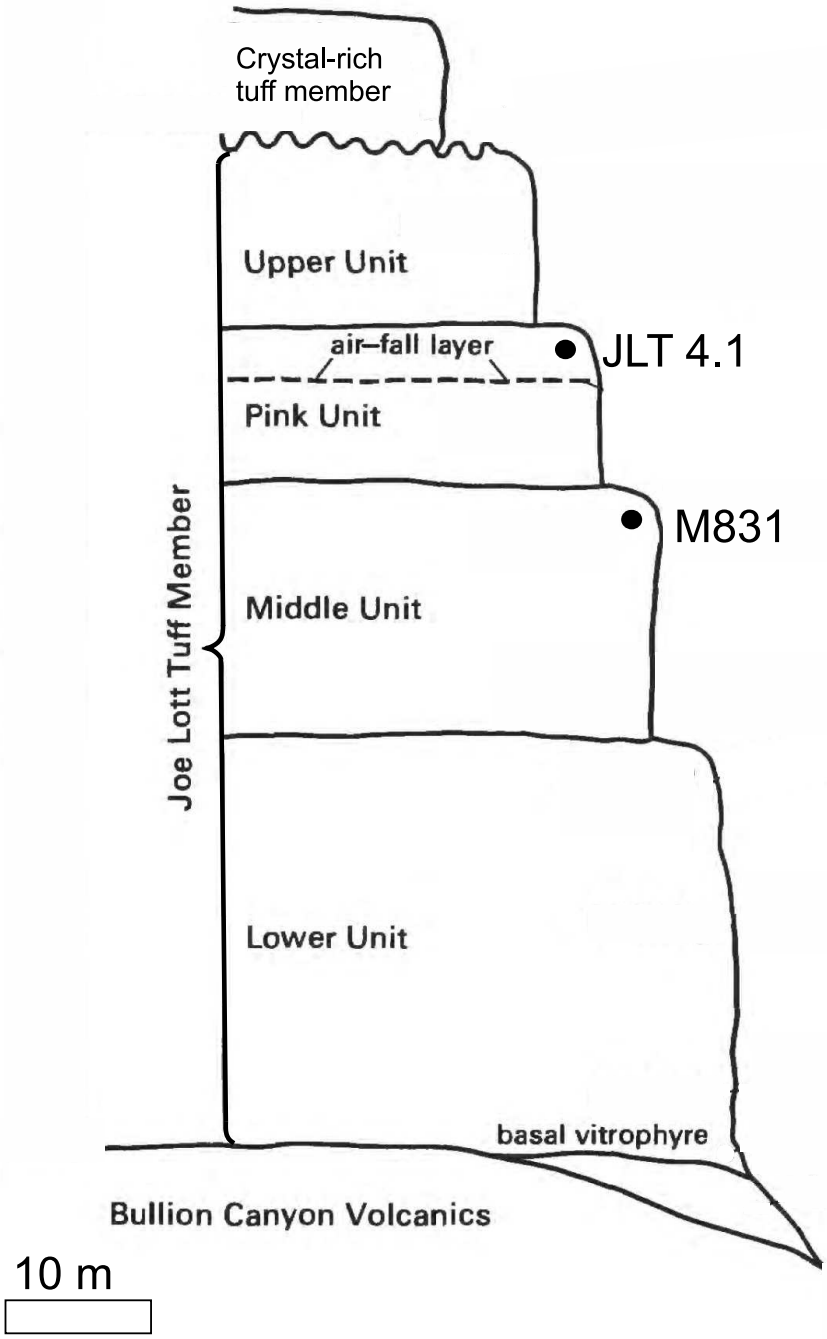

Figure 3

Click here to access/download;Figure;Fig.3.eps

Figure 4

Click here to access/download;Figure;Fig.4.eps

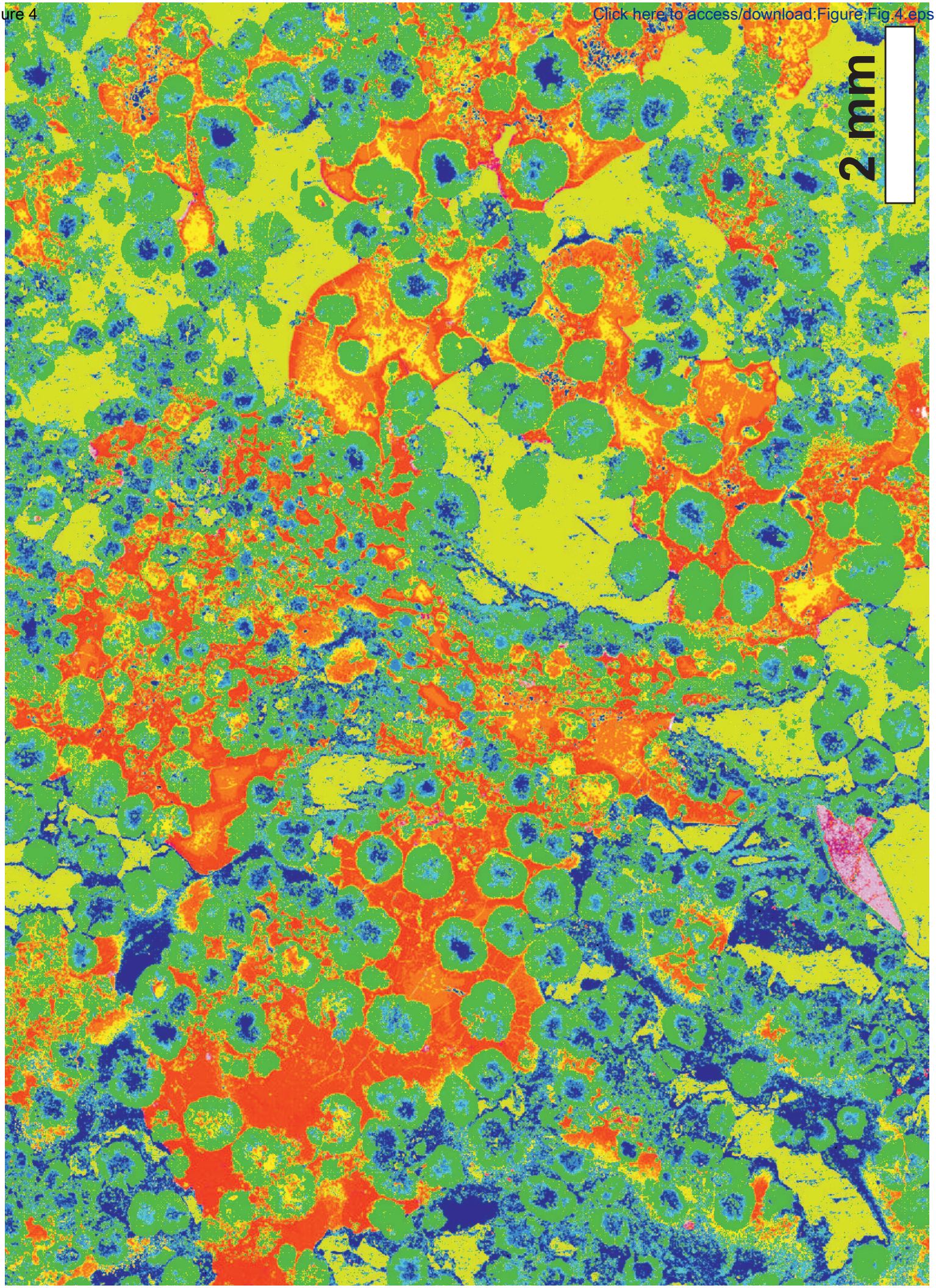

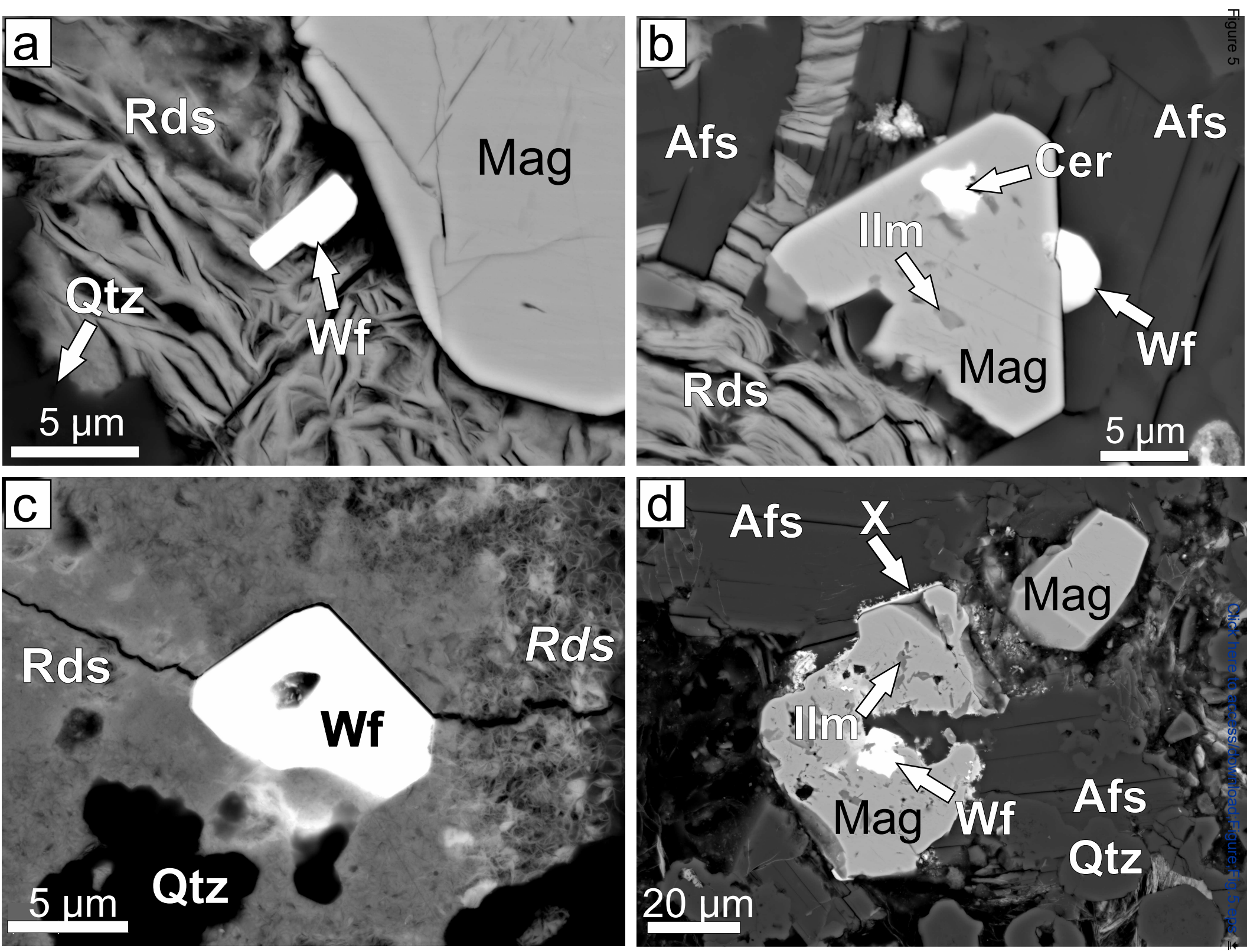

Figure 5

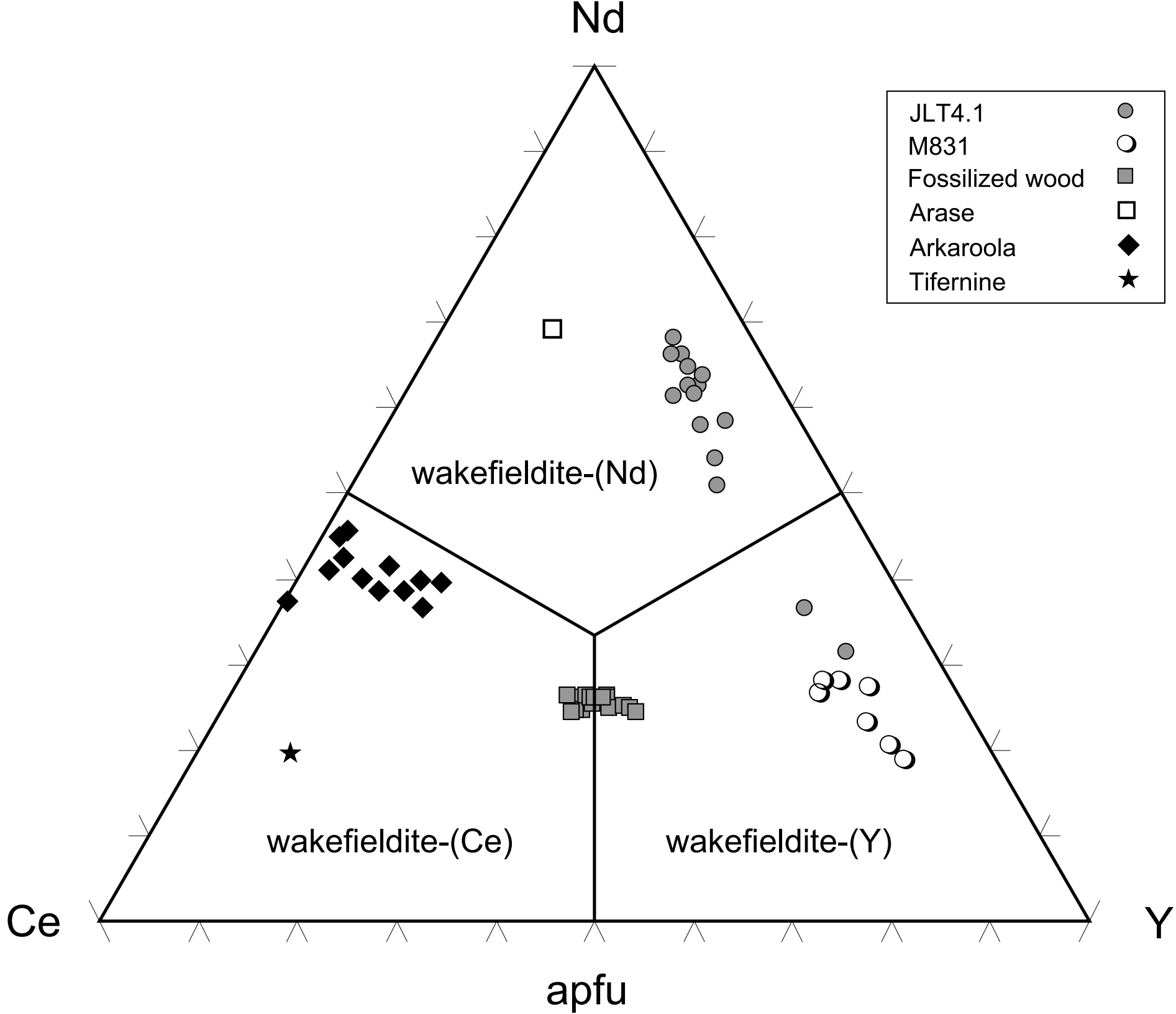

Figure 6

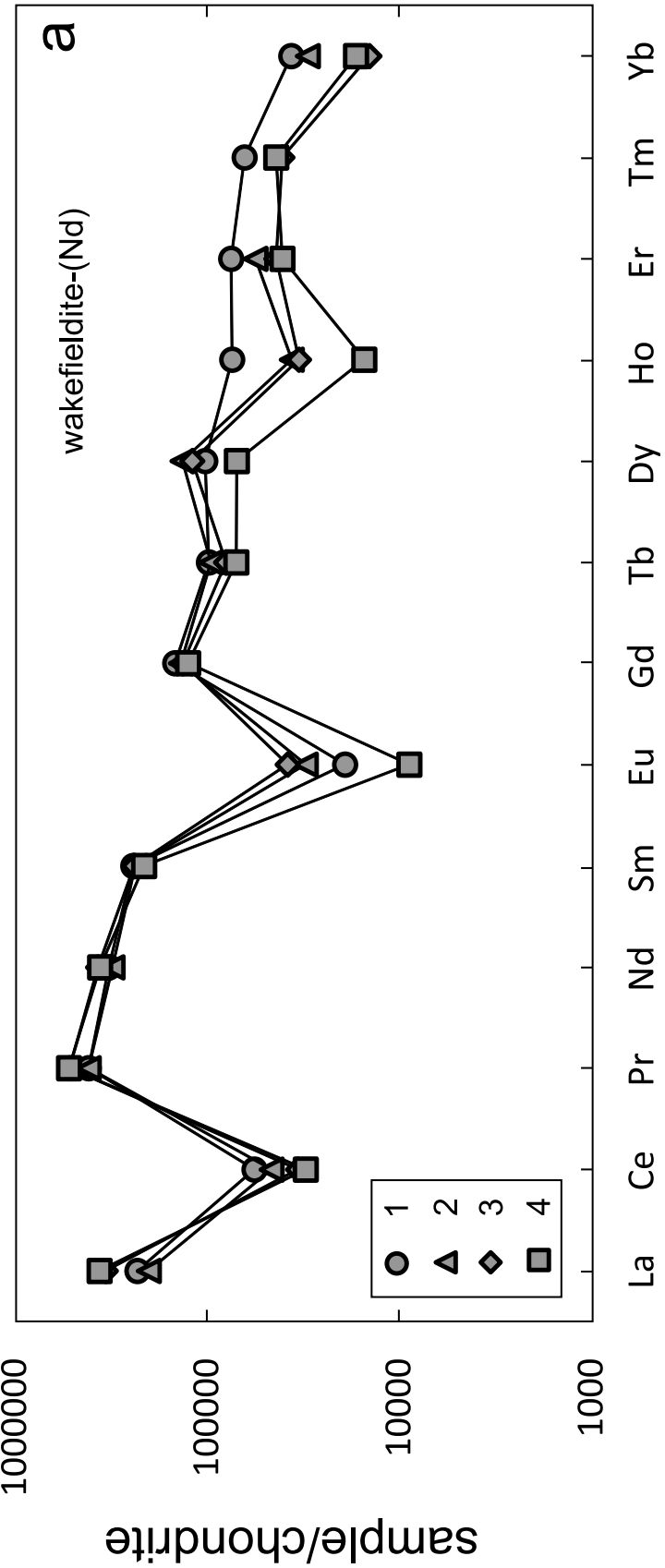

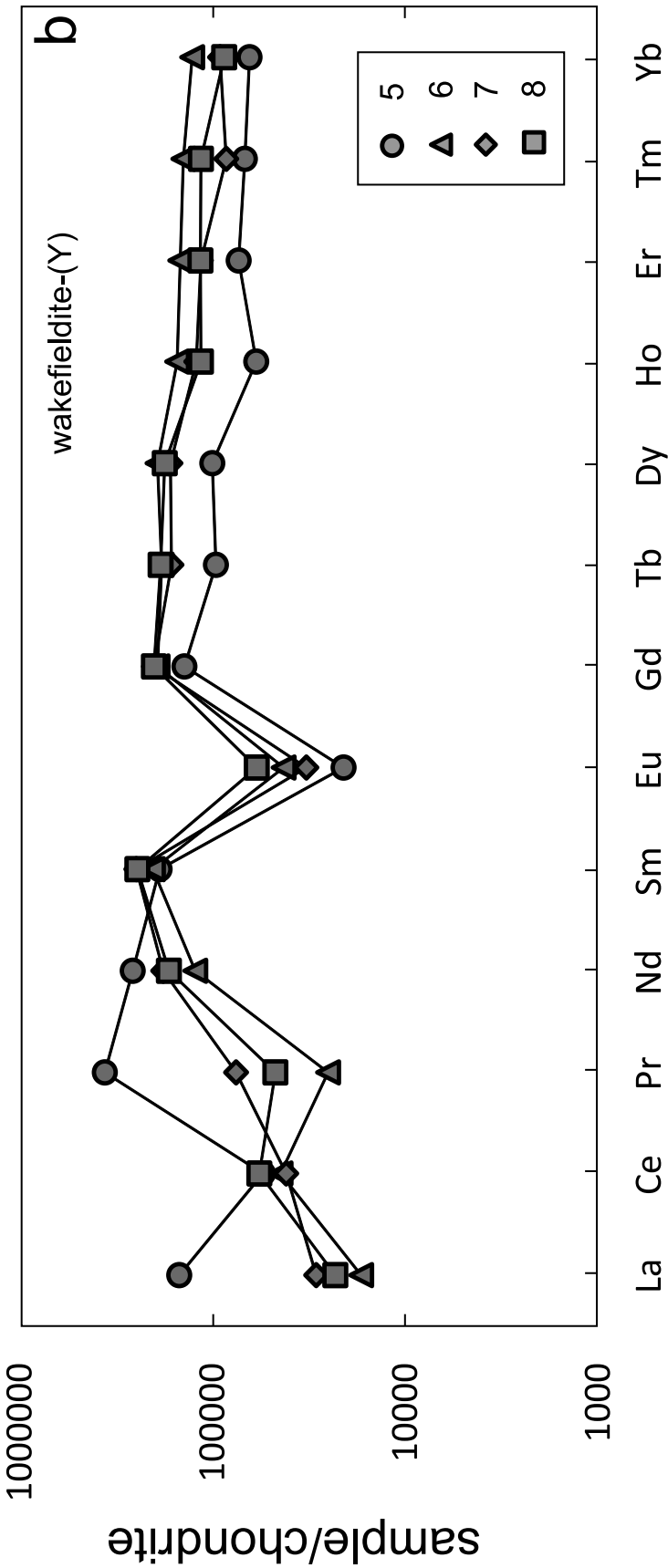

Figure 8

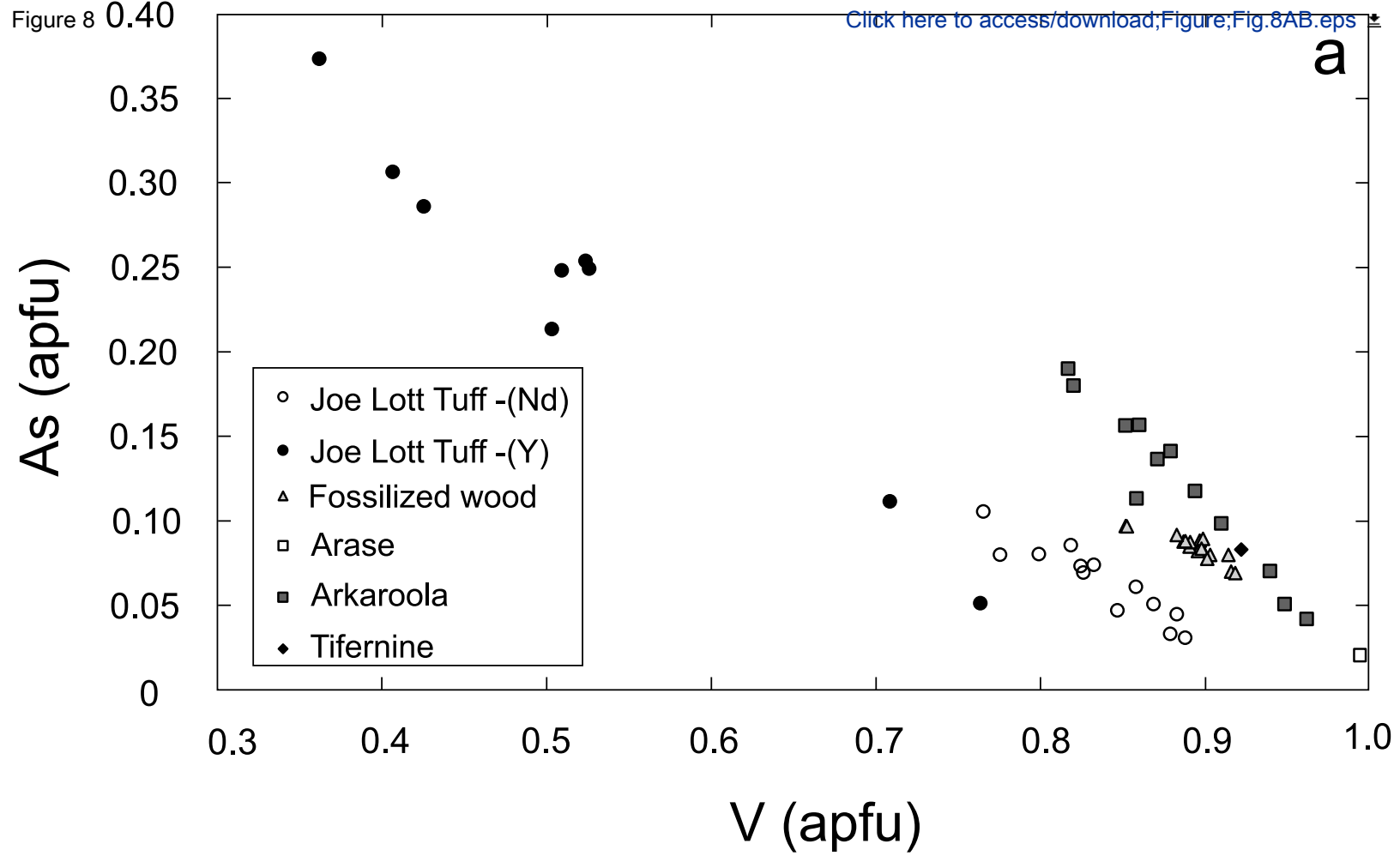

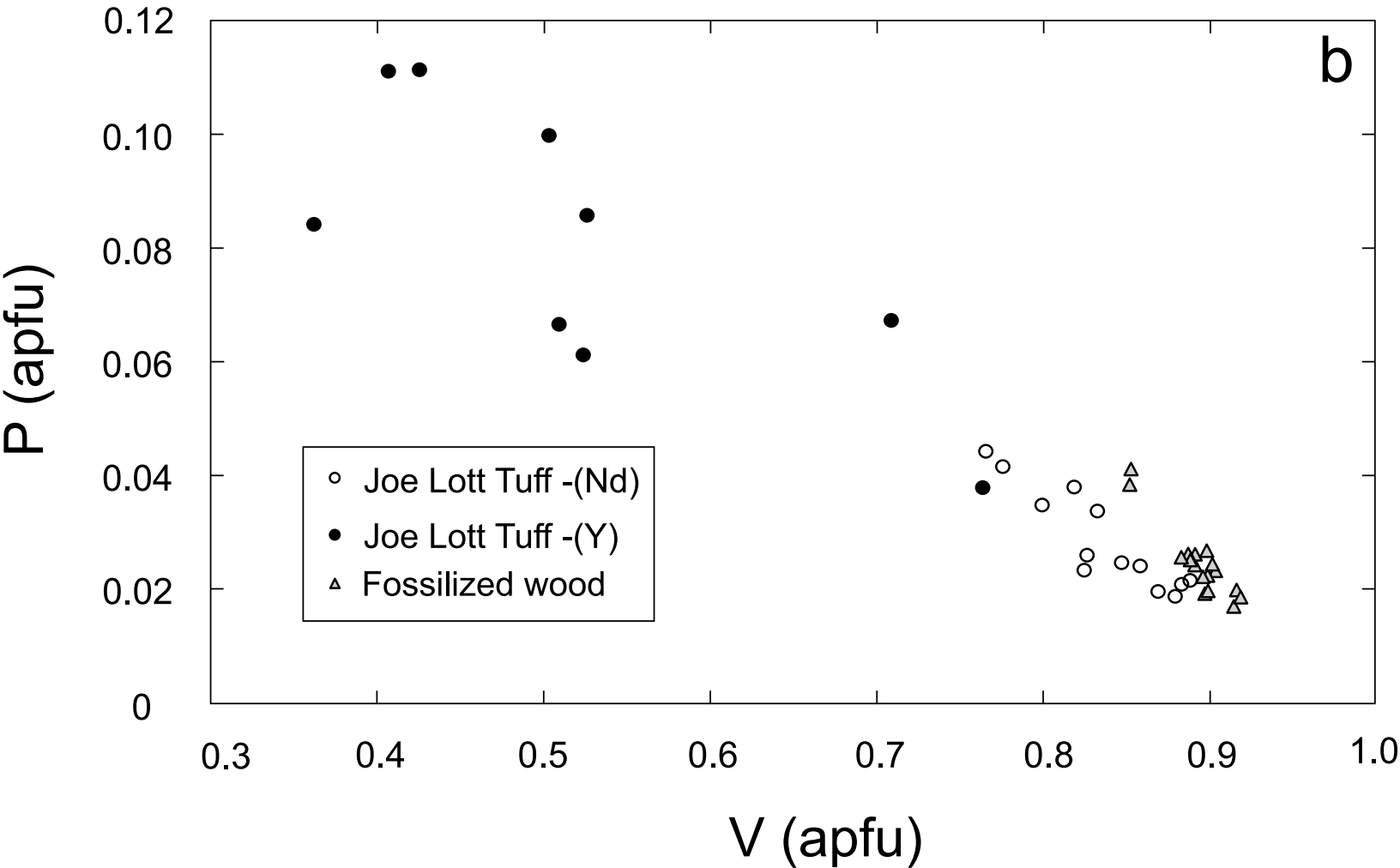

Figure 9

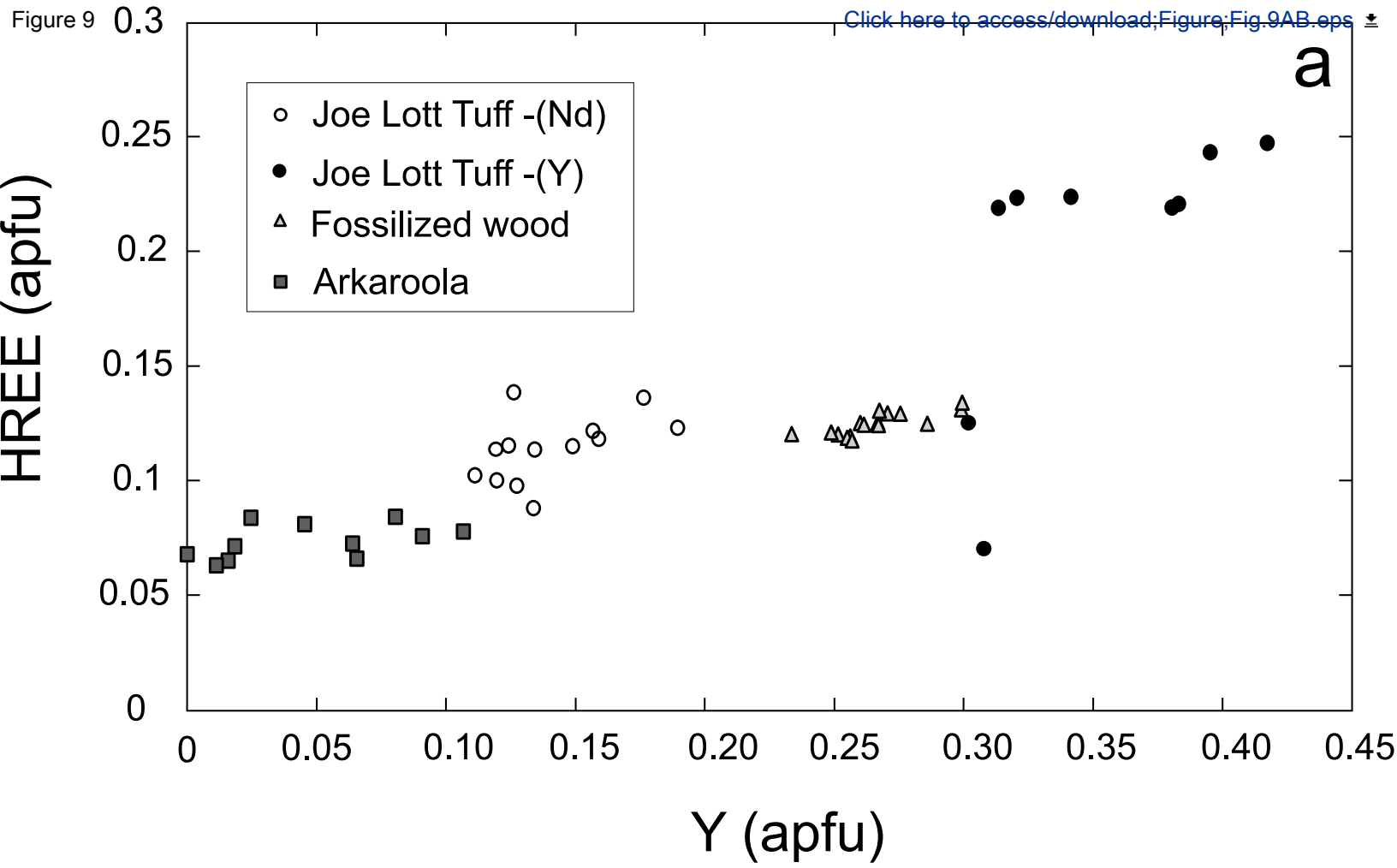

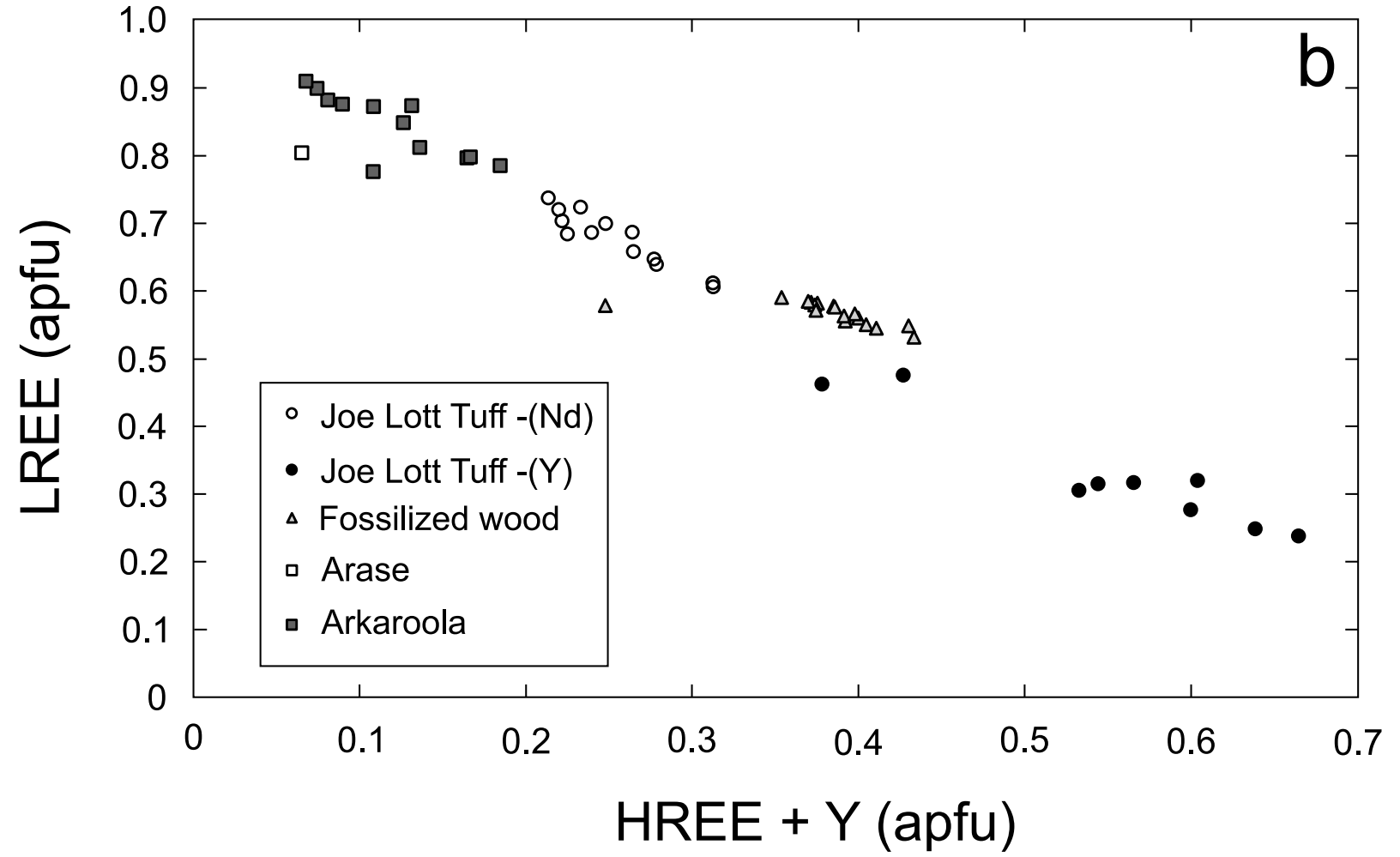

Figure 10

Click here to access/download;Figure;Fig.10AB.eps

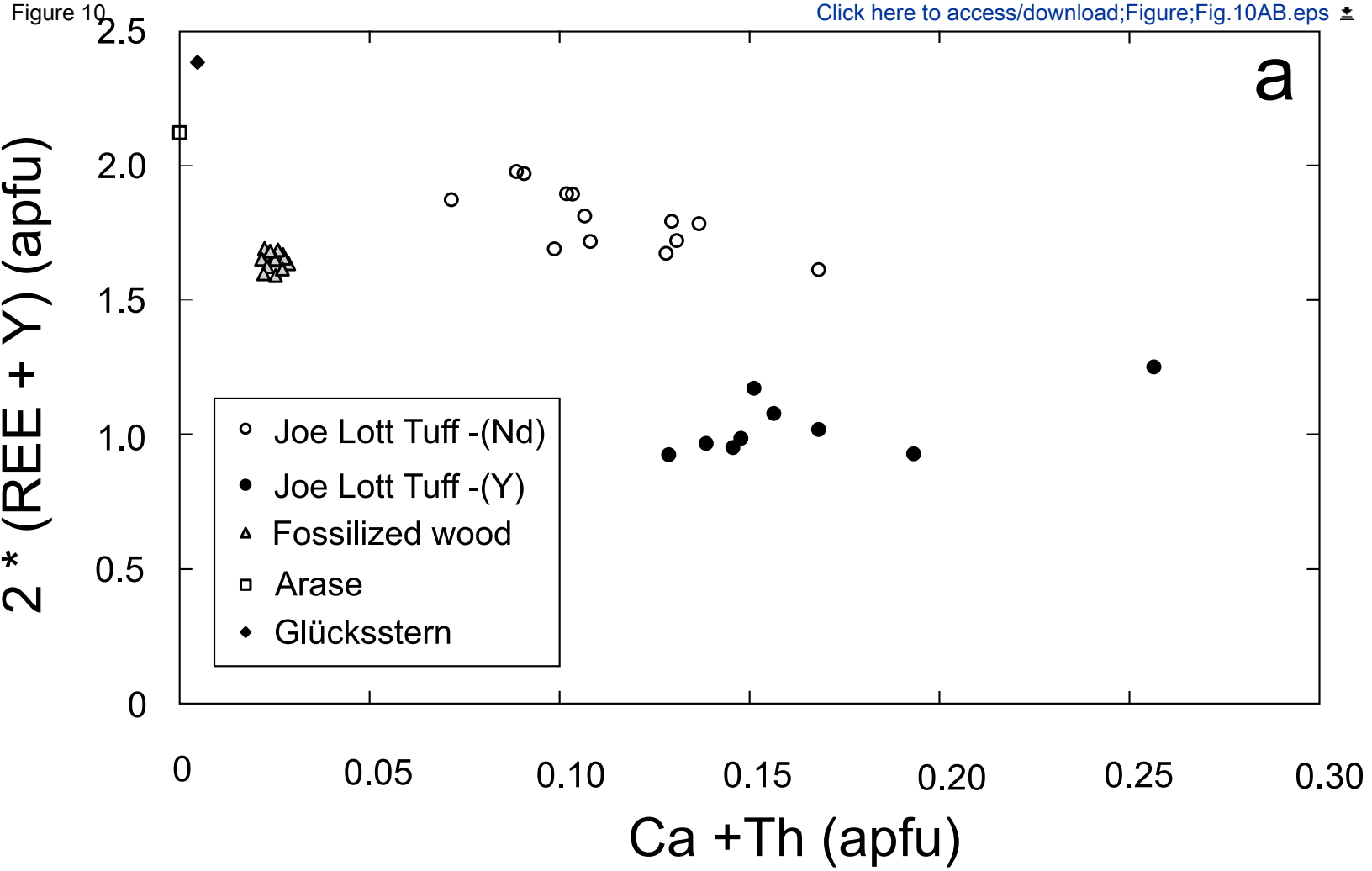

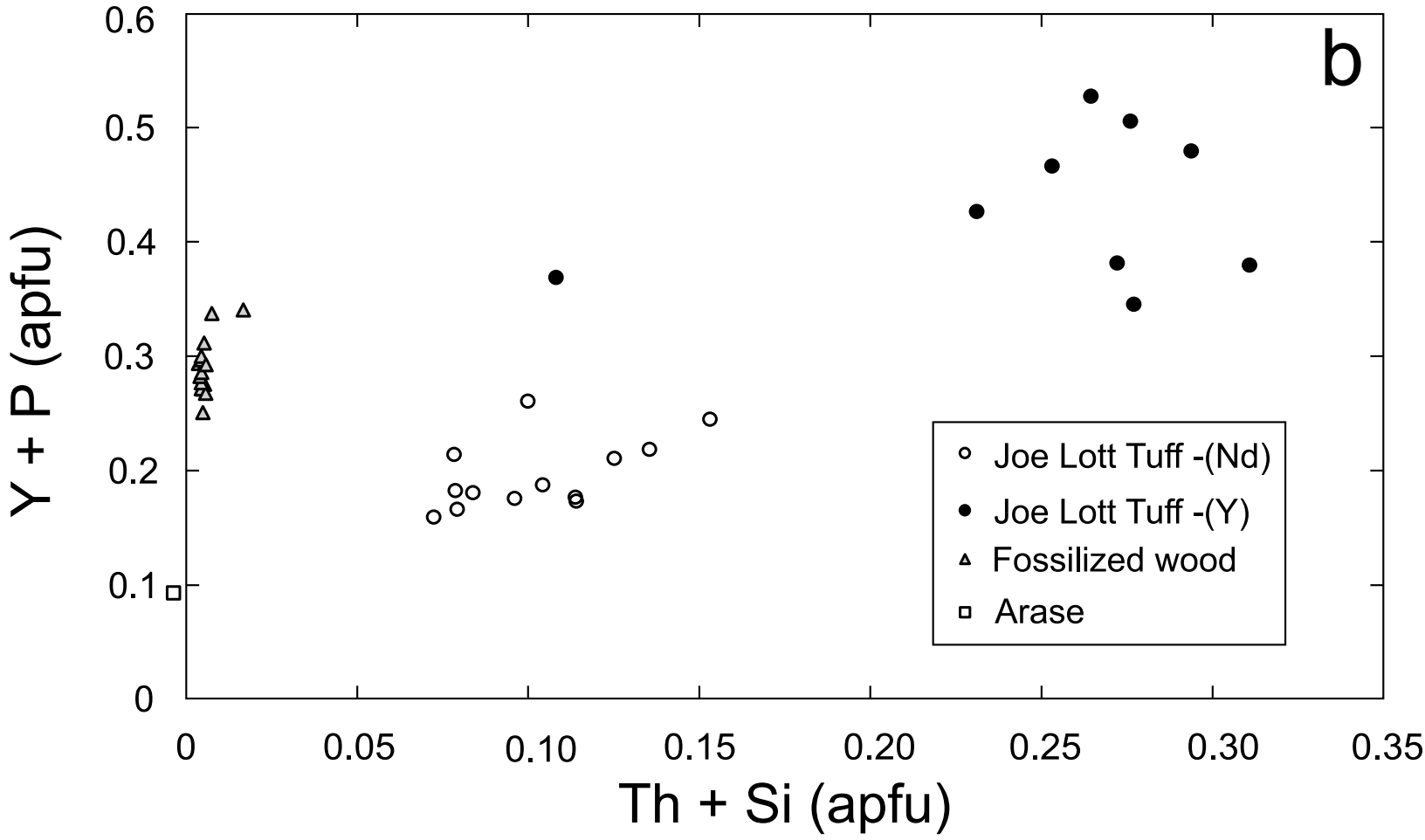

Figure 11

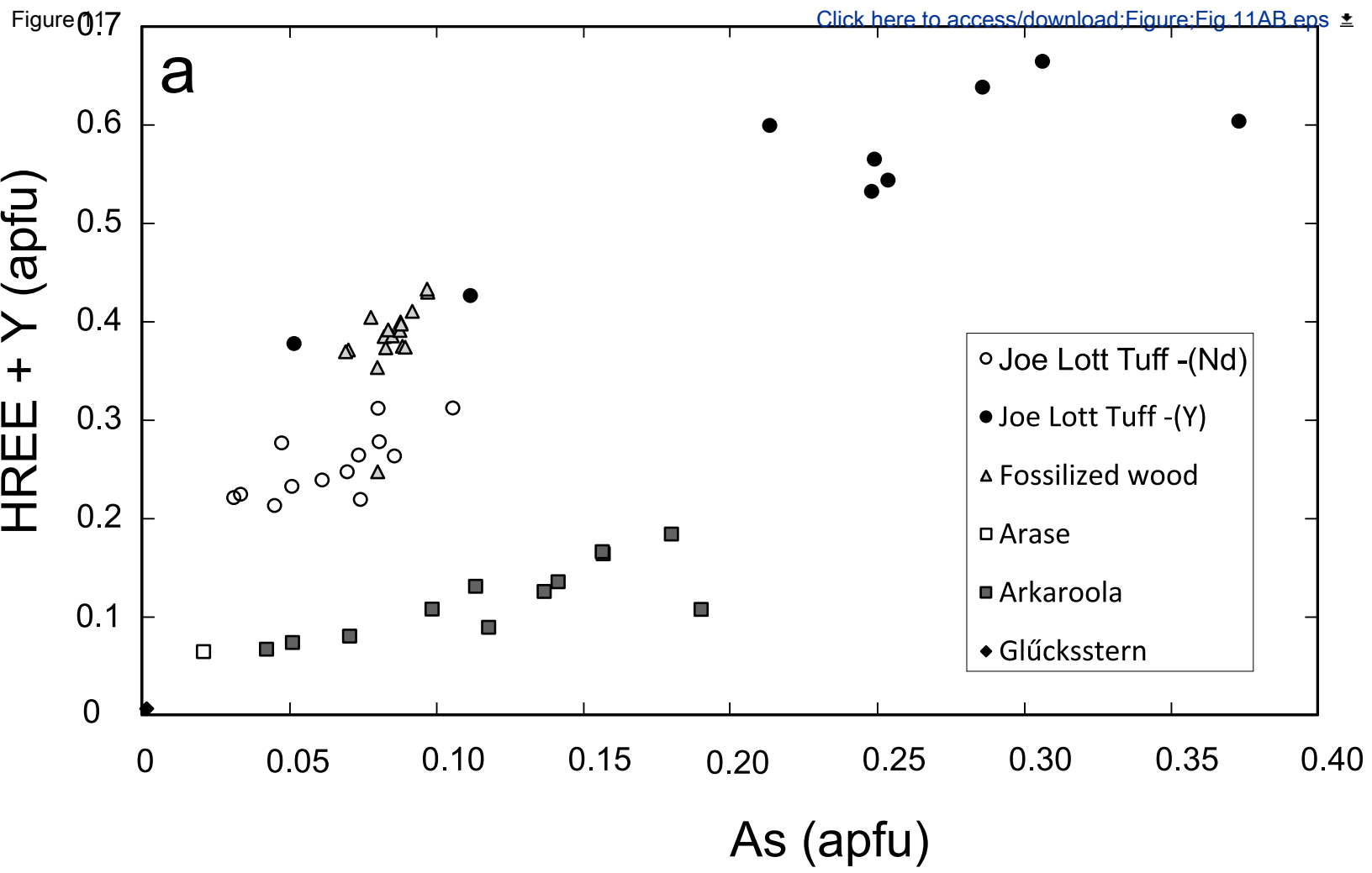

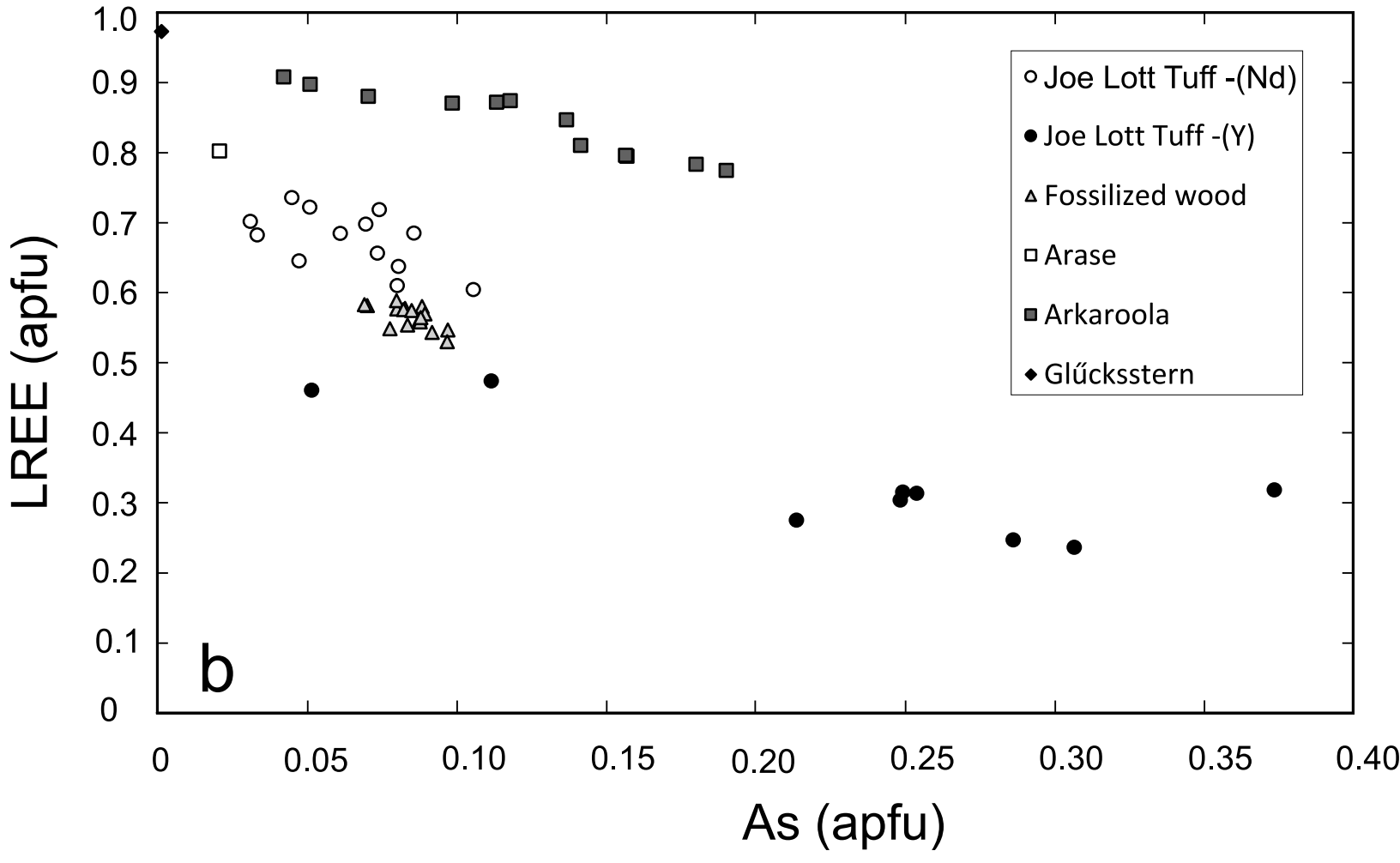

Table 1. EPMA method summary

Element/ x-ray line	Crystal	Peak Overlap Correction	Standard	Approx. Det. Limit (ppm)	Peak/Backg. Time (s)	Approx. Std Dev. wt%
Al Kα	TAP		Al_2O_3	200	30/30	0.02
As Lα	TAP		$ZnAs_2$	760	30/30	0.10
Bi Mα	LPET		Bi (metal)	740	30/30	0.07
Ca Kα	LPET		Wollastonite	160	20/20	0.02
Ce Lα	LPET		$CePO_4$	500	30/30	0.06
Dy Lα	LLIF		$DyPO_4$	1460	20/40	0.19
Er Lα	LLIF	Tb Lβ 4	$ErPO_4$	1450	20/40	0.14
Eu Lα	LLIF	Pr Lβ 2, Nd Lβ 3	$EuPO_4$	120	30/60	0.01
Gd Lα	LLIF	La Lγ 2, Ce Lγ	$GdPO_4$	1280	20/40	0.15
Ho Lα	LLIF	Gd Lβ	$HoPO_4$	160	30/60	0.02
Lu Mα	LTAP	Yb Mβ	$LuPO_4$	120	110/180	0.13
Lα Lα	LPET		$LaPO_4$	470	30/30	0.01
Mg Kα	TAP		MgO	240	20/20	0.02
Nb Lα	LPET		Nb (metal)	420	60/60	0.04
Nd Lα	LLIF	Ce Lβ	$NdPO_4$	1200	20/40	0.40
P Kα	TAP	Y Lβ	$CePO_4$	260	20/20	0.04
Pb Mα	LPET	Y Lγ 3	Crocoite	200	140/280	0.01
Pr Lα	LPET	La Lβ , V Kα	$PrPO_4$	290	30/60	0.06
S Kα	LPET		FeS_2	180	20/20	0.01
Si Kα	TAP		SiO_2	220	20/20	0.03
Sm Lα	LLIF	Ce Lβ 2	$SmPO_4$	1260	20/40	0.18
Sr Lα	TAP		$SrSO_4$	460	30/60	0.04
Tb Lα	LLIF		$TbPO_4$	1150	30/60	0.10
Th Mα	LPET		ThO_2	480	60/120	0.12
Ti Kα	LLIF		TiO_2	420	20/40	0.03
Tm Lα	LLIF	Sm Lγ , Dy Lβ 4	$TmPO_4$	270	30/60	0.02
U Mα	LPET	Th Mβ	UO_2	400	80/80	0.02
V Kα	LLIF		V (metal)	500	20/40	0.31
Y Lα	TAP		YPO_4	450	60/60	0.09
Yb Mα	LTAP	Dy Mγ	$YbPO_4$	400	120/120	0.03
Zr Lα	LPET		Zr (metal)	600	30/30	0.05

Table 2. Representative compositions of wakefieldite in the Joe Lott Tuff

	Wakefieldite-(Nd)				Wakefieldite-(Y)			
Sample	JLT4.1				JLT4.1	M831		
	1	2	3	4	5	6	7	8
wt.%								
CaO	1.04	1.28	0.99	1.92	4.80	0.61	0.68	0.84
SrO	0.10	bd	bd	0.07	bd	-	-	-
FeO*	-	-	-	-	-	0.05	0.43	bd
Y_2O_3	5.93	5.85	5.59	6.13	13.91	17.11	13.12	12.58
La_2O_3	7.82	10.62	8.74	10.39	4.22	0.47	0.64	0.70
Ce_2O_3	3.60	2.42	2.47	2.23	3.96	3.20	4.14	4.34
Pr_2O_3	5.79	5.66	5.43	6.01	4.16	0.28	0.53	0.50
Nd_2O_3	20.13	19.05	20.27	20.27	14.54	6.82	9.38	8.58
Sm_2O_3	4.63	3.59	4.61	3.87	3.43	3.71	4.46	4.07
Eu_2O_3	0.11	0.19	0.16	0.06	0.14	0.29	0.40	0.36
Gd_2O_3	3.23	2.86	3.38	3.04	3.37	4.67	4.89	4.55
Tb_2O_3	0.39	0.31	0.32	0.31	0.42	0.81	0.82	0.79
Dy_2O_3	3.23	2.97	3.42	2.08	2.97	5.75	5.27	5.00
Ho_2O_3	0.18	0.27	0.30	0.10	0.39	1.01	0.76	0.84
Er_2O_3	0.93	0.87	0.98	0.78	1.40	2.84	2.23	2.31
Tm_2O_3	0.11	0.17	bd	0.13	0.20	0.42	0.34	0.24
Yb_2O_3	0.38	0.29	0.34	0.33	1.26	2.52	1.71	1.69
SiO_2	1.40	1.20	1.04	0.88	1.51	3.21	3.00	3.42
TiO_2	bd	0.12	bd	0.11	bd	-	-	-
Nb_2O_5	bd	0.10	bd	bd	-	-	-	-
ThO_2	5.62	8.04	6.56	5.61	5.04	11.29	12.89	14.18
UO_2	bd	bd	bd	bd	bd	bd	bd	bd
PbO	bd	0.04	bd	bd	0.05	-	-	-
P_2O_5	0.72	0.54	0.68	0.62	1.95	5.73	3.15	3.36
V_2O_5	29.38	32.54	31.11	32.78	26.30	13.43	17.26	16.46
As_2O_5	3.13	1.56	2.80	1.45	5.24	12.80	10.58	10.15
SO_3	bd	bd	bd	bd	bd	0.10	0.05	0.06
Total	97.85	100.54	99.19	99.17	99.26	97.12	96.73	95.02
Formulae on the basis of 4 oxygens								
Ca	0.047	0.056	0.044	0.084	0.210	0.030	0.033	0.042
Fe^{2+}	-	-	-	-	-	0.002	0.017	0.000
Y	0.134	0.127	0.124	0.134	0.302	0.417	0.321	0.313
La	0.177	0.231	0.194	0.227	0.092	0.008	0.011	0.012
Ce	0.056	0.036	0.038	0.033	0.059	0.054	0.070	0.074
Pr	0.090	0.084	0.083	0.090	0.062	0.005	0.009	0.009
Nd	0.306	0.278	0.302	0.297	0.212	0.112	0.154	0.143
Sm	0.068	0.051	0.066	0.055	0.048	0.059	0.071	0.066
Eu	0.002	0.003	0.002	0.001	0.002	0.005	0.006	0.006

Gd	0.046	0.039	0.047	0.041	0.046	0.071	0.074	0.071
Tb	0.005	0.004	0.004	0.004	0.006	0.012	0.012	0.012
Dy	0.044	0.039	0.046	0.027	0.039	0.085	0.078	0.075
Er	0.013	0.012	0.014	0.011	0.019	0.044	0.035	0.037
Yb	0.005	0.004	0.004	0.004	0.016	0.035	0.024	0.024
Ti	0.000	0.002	0.000	0.001	0.000	-	-	-
Th	0.054	0.075	0.062	0.052	0.047	0.118	0.135	0.151
U	0.000	0.000	0.000	0.000	0.000	0.000	0.000	0.000
Sum	1.048	1.039	1.031	1.060	1.158	1.055	1.049	1.036
V	0.826	0.879	0.858	0.888	0.708	0.407	0.524	0.509
Si	0.060	0.049	0.043	0.036	0.062	0.147	0.138	0.160
As	0.070	0.033	0.061	0.031	0.112	0.307	0.254	0.248
P	0.026	0.019	0.024	0.022	0.067	0.111	0.061	0.067
Sum	0.981	0.980	0.986	0.976	0.949	0.971	0.976	0.984
S	0.000	0.000	0.000	0.000	0.000	0.003	0.002	0.002
Σ cations	2.03	2.02	2.02	2.04	2.11	2.03	2.03	2.02

FeO*, all Fe as Fe^{2+}. bd, below detection. Dash - not determined

Supplementary Table 1. Compositions of wakefieldite in Joe Lott Tuff

	Wakefieldite-(Nd)							-
Sample	JLT 4.1							
	1	2	3	4	5	6	7	8
wt.%								
P_2O_5	1.28	0.98	0.72	1.11	0.54	0.70	0.59	0.62
V_2O_5	28.37	28.87	29.38	26.54	32.54	30.85	32.05	28.11
As_2O_5	4.95	3.68	3.13	3.47	1.56	2.18	2.06	3.17
Nb_2O_5	bd	0.09	bd	0.13	0.10	0.10	bd	0.09
SiO_2	1.34	2.12	1.40	1.71	1.20	1.60	0.77	1.29
TiO_2	bd	0.03	bd	0.68	0.12	0.10	0.05	0.85
ThO_2	5.91	5.92	5.62	8.67	8.04	7.24	5.27	6.56
UO_2	bd	bd	bd	bd	bd	bd	bd	bd
SO_3	bd	bd	bd	bd	bd	bd	bd	bd
Y_2O_3	8.72	7.03	5.93	7.49	5.85	7.19	5.01	5.34
La_2O_3	6.58	6.83	7.82	5.75	10.62	8.77	9.80	7.81
Ce_2O_3	4.15	3.29	3.60	3.38	2.42	2.29	2.41	2.58
Pr_2O_3	4.74	5.13	5.79	4.74	5.66	5.10	6.02	4.81
Nd_2O_3	18.19	19.34	20.13	17.41	19.05	18.63	21.66	17.89
Sm_2O_3	4.43	4.51	4.63	4.32	3.59	4.18	4.55	4.18
Eu_2O_3	0.13	0.18	0.11	0.21	0.19	0.27	0.20	0.34
Gd_2O_3	3.56	3.58	3.23	3.33	2.86	3.29	3.26	3.07
Tb_2O_3	0.43	0.33	0.39	0.42	0.31	0.38	0.34	0.37
Dy_2O_3	3.05	3.41	3.23	4.01	2.97	3.43	2.82	4.79
Ho_2O_3	0.49	0.14	0.18	0.24	0.27	0.15	0.06	0.26
Er_2O_3	1.45	1.00	0.93	1.08	0.87	1.09	0.79	0.93
Tm_2O_3	0.19	0.15	0.11	bd	0.17	0.27	bd	bd
Yb_2O_3	0.72	0.57	0.38	0.59	0.29	0.51	0.28	0.41
CaO	2.59	0.94	1.04	0.86	1.28	0.89	0.91	1.33
FeO*	-	-	-	-	-	-	-	-
SrO	0.07	0.08	0.10	bd	bd	0.08	0.11	bd
PbO	0.05	bd	bd	bd	0.04	0.04	bd	bd
Total	101.39	98.20	97.85	96.14	100.54	99.33	99.01	94.80
	Formulae on the basis of 4 oxygens							
Ca	0.113	0.042	0.047	0.041	0.056	0.040	0.041	0.063
Fe^{2+}	-	-	-	-	-	-	-	-
Y	0.189	0.157	0.134	0.176	0.127	0.159	0.111	0.126
La	0.143	0.152	0.177	0.135	0.231	0.194	0.217	0.184
Ce	0.062	0.050	0.056	0.055	0.036	0.035	0.037	0.042
Pr	0.071	0.078	0.090	0.076	0.084	0.077	0.091	0.078
Nd	0.265	0.289	0.306	0.275	0.278	0.276	0.322	0.284
Sm	0.062	0.065	0.068	0.066	0.051	0.060	0.065	0.064
Eu	0.002	0.003	0.002	0.003	0.003	0.004	0.003	0.005

Gd	0.048	0.050	0.046	0.049	0.039	0.045	0.045	0.045
Tb	0.006	0.005	0.005	0.006	0.004	0.005	0.005	0.005
Dy	0.040	0.046	0.044	0.057	0.039	0.046	0.038	0.068
Er	0.020	0.014	0.013	0.016	0.012	0.015	0.011	0.014
Yb	0.009	0.007	0.005	0.008	0.004	0.006	0.004	0.006
Ti	0.000	0.001	0.000	0.023	0.001	0.028	0.000	0.003
Th	0.055	0.056	0.054	0.087	0.075	0.068	0.050	0.066
U	0.000	0.000	0.000	0.000	0.000	0.000	0.000	0.000
Sum	1.086	1.016	1.048	1.074	1.040	1.059	1.040	1.054
V	0.765	0.799	0.826	0.775	0.879	0.847	0.883	0.824
Si	0.055	0.089	0.060	0.076	0.049	0.066	0.032	0.057
As	0.106	0.081	0.070	0.080	0.033	0.047	0.045	0.074
P	0.044	0.035	0.026	0.042	0.019	0.025	0.021	0.023
Sum	0.970	1.003	0.981	0.973	0.980	0.985	0.980	0.978
S	0.000	0.000	0.000	0.000	0.000	0.000	0.000	0.000
Σ cations	2.06	2.02	2.03	2.02	2.02	2.02	2.02	2.03

FeO*, all Fe as Fe^{2+}. bd, below detection. Dash - not determined

					Wakefieldite-(Y) JLT 4.1		M831
9	10	11	12	13	14	15	16
0.55	0.68	0.94	1.01	0.62	1.95	1.16	5.73
31.34	31.11	29.72	27.93	32.78	26.3	30.01	13.43
2.32	2.8	3.35	3.70	1.45	5.24	2.56	12.80
bd	bd	bd	0.33	bd	-	-	-
0.95	1.04	1.01	0.94	0.88	1.51	5.21	3.21
bd	bd	bd	0.68	0.11	bd	bd	-
5.14	6.56	5.26	4.59	5.61	5.04	8.76	11.29
bd	bd	bd	bd	bd	bd	bd	bd
bd	bd	bd	bd	bd	bd	bd	0.10
5.34	5.59	5.30	6.31	6.13	13.91	15.02	17.11
9.66	8.74	8.16	7.15	10.39	4.22	7.99	0.47
2.45	2.47	2.82	2.86	2.23	3.96	3.21	3.20
5.96	5.43	5.98	5.45	6.01	4.16	4.30	0.28
20.78	20.27	21.50	20.02	20.27	14.54	11.96	6.82
4.36	4.61	4.86	4.14	3.87	3.43	2.05	3.71
0.26	0.16	0.16	0.12	0.06	0.14	bd	0.29
3.25	3.38	3.32	3.21	3.04	3.37	1.92	4.67
0.35	0.32	0.32	0.37	0.31	0.42	0.21	0.81
3.56	3.42	2.34	2.69	2.08	2.97	1.57	5.75
0.22	0.30	0.10	0.28	0.10	0.39	0.23	1.01
0.84	0.98	0.84	1.08	0.78	1.40	0.99	2.84
0.12	bd	0.11	0.18	0.13	0.20	0.19	0.42
0.28	0.34	0.39	0.57	0.33	1.26	0.91	2.52
0.88	0.99	1.16	0.53	1.92	4.80	1.26	0.61
-	-	-	-	-	-	-	0.05
bd	bd	0.09	0.07	0.07	bd	0.08	-
bd	bd	bd	bd	bd	0.05	0.07	-
98.61	99.19	97.73	94.21	99.17	99.26	99.66	97.12
0.040	0.044	0.053	0.025	0.084	0.210	0.052	0.030
-	-	-	-	-	-	-	0.002
0.119	0.124	0.120	0.149	0.134	0.302	0.308	0.417
0.216	0.194	0.184	0.169	0.227	0.092	0.164	0.008
0.038	0.038	0.044	0.046	0.033	0.059	0.045	0.054
0.091	0.083	0.092	0.088	0.090	0.062	0.060	0.005
0.311	0.302	0.325	0.317	0.297	0.212	0.164	0.112
0.063	0.066	0.071	0.063	0.055	0.048	0.027	0.059
0.004	0.002	0.002	0.002	0.001	0.002	0.000	0.005

0.045	0.047	0.047	0.047	0.041	0.046	0.025	0.071
0.005	0.004	0.004	0.005	0.004	0.006	0.003	0.012
0.048	0.046	0.032	0.038	0.027	0.039	0.019	0.085
0.012	0.014	0.012	0.016	0.011	0.019	0.013	0.044
0.004	0.004	0.005	0.008	0.004	0.016	0.011	0.035
0.001	0.001	0.001	0.023	0.003	0.000	0.000	-
0.049	0.062	0.051	0.046	0.052	0.047	0.077	0.118
0.000	0.000	0.000	0.000	0.000	0.000	0.000	0.000
1.045	1.032	1.043	1.044	1.063	1.158	0.968	1.055
0.869	0.858	0.832	0.818	0.888	0.708	0.763	0.407
0.040	0.043	0.043	0.042	0.036	0.062	0.201	0.147
0.051	0.061	0.074	0.086	0.031	0.112	0.052	0.307
0.020	0.024	0.034	0.038	0.022	0.067	0.038	0.111
0.979	0.986	0.983	0.984	0.976	0.949	1.053	0.971
0.000	0.000	0.000	0.000	0.000	0.000	0.000	0.003
2.02	2.02	2.02	2.00	2.04	2.11	2.02	2.03

17	18	19	20	21	22	
3.15	3.36	5.72	5.17	4.36	4.27	
17.26	16.46	13.99	16.69	17.12	11.76	
10.58	10.15	11.9	8.96	10.26	15.34	
-	-	-	-	-	-	
3.00	3.42	3.68	4.06	2.46	2.86	
-	-	-	-	-	-	
12.89	14.18	10.22	10.49	11.06	11.34	-
bd	bd	bd	bd	bd	bd	
0.05	0.06	0.10	0.06	0.08	0.18	
13.12	12.58	16.14	15.67	13.80	15.45	
0.64	0.70	0.46	0.50	0.68	0.81	
4.14	4.34	3.31	3.75	3.66	2.99	
0.53	0.50	0.33	0.49	0.60	0.85	
9.38	8.58	7.18	8.33	9.60	10.02	
4.46	4.07	3.80	3.86	4.49	4.52	
0.40	0.36	0.32	0.34	0.35	0.22	
4.89	4.55	4.94	4.34	4.85	4.89	
0.82	0.79	0.80	0.70	0.77	0.72	
5.27	5.00	5.70	5.25	5.27	4.92	
0.76	0.84	0.99	0.79	0.77	0.80	
2.23	2.31	2.63	2.41	2.20	2.21	
0.34	0.24	0.43	0.30	0.36	0.25	
1.71	1.69	2.16	2.05	1.68	1.80	
0.68	0.84	0.64	0.75	0.79	0.62	
0.43	bd	0.07	bd	bd	bd	
-	-	-	-	-	-	
-	-	-	-	-	-	
96.73	95.02	95.51	94.96	95.21	96.82	
0.033	0.042	0.032	0.037	0.039	0.031	
0.017	0.000	0.003	0.000	0.000	0.000	
0.321	0.313	0.395	0.380	0.341	0.383	
0.011	0.012	0.008	0.008	0.012	0.014	
0.070	0.074	0.056	0.063	0.062	0.051	
0.009	0.009	0.006	0.008	0.010	0.014	
0.154	0.143	0.118	0.136	0.159	0.167	
0.071	0.066	0.060	0.061	0.072	0.073	
0.006	0.006	0.005	0.005	0.006	0.003	

0.074	0.071	0.075	0.066	0.075	0.075
0.012	0.012	0.012	0.010	0.012	0.011
0.078	0.075	0.084	0.077	0.079	0.074
0.035	0.037	0.041	0.038	0.035	0.035
0.024	0.024	0.030	0.029	0.024	0.026
-	-	-	-	-	-
0.135	0.151	0.107	0.109	0.117	0.120
0.000	0.000	0.000	0.000	0.000	0.000
1.049	1.036	1.032	1.026	1.043	1.077
0.524	0.509	0.425	0.503	0.526	0.362
0.138	0.160	0.169	0.185	0.114	0.133
0.254	0.248	0.286	0.214	0.249	0.374
0.061	0.067	0.111	0.100	0.086	0.084
0.976	0.984	0.992	1.002	0.975	0.953
0.002	0.002	0.003	0.002	0.003	0.006
2.03	2.02	2.02	2.03	2.02	2.03

Wakefieldite occurrences

Canada

Wakefieldite-(Ce). veins in porphyritic trachyte, Osoyoos Mining Division, Yellow Lake, British Columbia (Howard *et al*., 1995)

Wakefieldite-(Y), in zoned granite pegmatite, near Wakefield Lake, Quebec (Miles *et al*., 1971)

USA

Wakefieldite-(Y), Huron River uranium prospect, Baraga County, Michigan (Carlson *et al*., 2007)

Wakefieldite-(Y), lining voids in euxenite-(Y), White Tank Mountains, Maricopa County, Arizona (Anthony *et al*., 1995)

Wakefieldite-(Nd), wakefieldite-(Y), in Joe Lott rhyolitic ignimbrite, Utah (this paper)

Wakefieldite-(Y), as rims on chernovite-(Y), Taylor Creek Tin District, Sierra County, New Mexico (Foord & Hlava, 1991)

Scotland

Wakefieldite-(Ce) in reduction spots in sandstone, Gamrie Bay, Banffshire (Van Panhuys-Sigler *et al.*, 2018)

Germany

Wakefieldite-(La), in hydrothermal barytes veins, Glűcksstern Mine, Friedrichroda, Thuringia (Witzke *et al*., 2008).

Wakefieldite-(Ce) and wakefieldite-(Nd), manganese mine, Ilfeld, Harz (Gröbner *et al*., 2011)

Wakefieldite-(La), Bellerberg volcano, Mayen-Koblenz, Rhineland-Palatinate (Blass, 2010).

Reported in mindat.org.: accessed 25/12/2018

Wakefieldite-(Ce), Clara Mine, Rankach Valley, Baden-Württenberg (Kolitsch *et al*., 2005)

Austria

Wakefieldite-(Ce), wakefieldite-(Y), Obernberger Tribulaun, North Tyrol (Kolitsch *et al*., 2018)

Czech Republic

Wakefieldite-(Ce,Y), in silicified wood near Studenec (Matysova *et al*., 2016)

Probable wakefieldite-(Ce), in teschenite sill, Krmelin, Frýdek-Místek, Moravia-Silesia (Matýsek, 2013)

Italy

Wakefieldite-(La), Cerchiara Mine, La Spezia Province, Liguria (reported in mindat.org; accessed 19/1/2018)

Wakefieldite-(Ce), Pianciano, Roman Volcanic Province. Fluor-ore-carbonatite units interbedded with silicate volcanics (Stoppa *et al*., 2016).

Wakefieldite-(Y), on quartz-calcite matrix, Borgata Oberti, Montaldo di Mondovi (Cadoni *et al*., 2011)

Morocco

Wakefieldite-(Ce), quartzose dyke?, Tifernine plateau (Baudracco-Gritti *et al*., 1987)

Egypt

Wakefieldite-(Y), in silver-gold mineralization associated with uranium bearing minerals and base metal sulphide, El Sheik Soliman area, south Sinai (Sallam *et al*., 2014).

Democratic Republic of the Congo

Wakefieldite-(Ce), Kobokobo pegmatite, Sud-Kivu (Deliens & Piret, 1977, 1986)

Namibia

Wakefieldite-(Y), mineralized quartz vein, Garnsberg region (Bezing *et al*., 2014)

Jordan

Wakefieldite-(Ce), marbles, Tulul Al Hamman area (Khoury *et al*., 2015)

Japan

Wakefieldite-(Nd), Arase stratiform ferromanganese deposit, Kochi Prefecture (Moriyama *et al*., 2010).

Australia

Wakefieldite-(Ce), diopside-titanite veins, Arkaroola, Flinders Range, South Australia (Bakker & Elburg, 2006),

References

Anthony, J.W., Williams, S.A., Bideaux, R.A., Grant, R.W. (1995): Mineralogy of Arizona, 3rd edition. University of Arizona Press, Tucson.

Bakker, R.J. & Elburg, M.A. (2006): A magmatic-hydrothermal transition in Arkaroola

(northern Flinders Ranges, South Australia): from diopside-titanite pegmatites to hematite-quartz growth. *Contrib. Mineral. Petrol.*, **152**, 541-569.

Bezing, L. von, Bode, R., Jahn, S. (2014): Namibia Minerals and Localities. 2nd edition Schloss Freudenstein, Bode Verlag GmbH, Haltern: 608 pp.

Blass, G. (2010): Die neuen Mineralienfunde aus der Vulkaneifel, Mineralien-Welt, 5.

Cadoni, M., Ciriotti, M.E., Ferraris, G. (2011): Wakefieldite-(Y) from Montaldo di Mondovi (Italy): new data and crystal structure. *Rend. Lincei*, **22**, 307-314.

Carlson, S.M., Robinson, G.W., Elder, M.J., Jaszczak, J.A., Bornhorst, T.J. (2007): Greenockite and associated uranium-vanadium minerals from the Huron River uranium prospect, Baraga County, Michigan. *Rocks and Minerals*, **82**, 298-308.

Deliens, M. & Piret, P. (1977): La kusuïte (Ce^{3+}, Pb^{2+}, Pb^{4+})VO_4, nouveau minéral. *Bull.Soc. Fran. Minéral. Cristall.*, **100**, 39-41.

Foord, E.E. & Hlava, P.F. (1991): Rare-earth arsenates and other rare-earth minerals from the Black Range Tin District, Sierra and Catron Counties, New Mexico. *New Mexico Geology*, **13**, 40-41.

Gröbner, J., Kolitsch, U., Wesiger, J. (2011): New finds of vanadate and rare-earth minerals from the manganese mine Ilfeld, Harz. *Mineral-Welt*, **22** (1), 41-49. (in German).

Howard, D.G., Tschernich, R.W., Klein, G.L. (1995): Occurrence of wakefieldite-(Ce) with zeolites at Yellow Lake, British Columbia, Canada. *N. Jb.Mineral. Mh.*, **3**, 127–132.

Khoury, H.N., Sokol, E.V., Clark, I.D. (2015): Calcium uranium oxide minerals from central Jordan: assemblages, chemistry, and alteration products. *Can. Mineral.*,**53**, 61-82.

Kolitsch, U., Gröbner, J., Blaß, G., Graf, H.-W., Pring, A. (2005): Neufunde aus der Grube Clara im mittleren Schwarzwald (II). *Lapis*, **30 (9),** 35-39.

Kolitsch, U., Schachinger, T., Auer, C. (2018): Pp. 206-213 *in* F. Walter *et al*. *Neue Mineralfunde aus Österreich* **LXVII**.

Matýsek D. (2013): Projevy mobilizace prvků vzácných zemin (REE) v podbeskydských těšínitech. *Acta Musei Moraviae: Scientiae geol.,* **98**, 101–113.

Matysova, P., Götze, J., Leichmann, J., Škoda, R., Strnad, L., Drahota, P., Grygar, T. (2016): Cathodoluminescence and LA-ICP-MS chemistry of silicified wood enclosing wakefieldite – REEs and V migration during complex diagenetic evolution. *Eur.J.Mineral.,* **28**, 869-887.

Miles, N.M., Hogarth, D.D., Russell, D.S. (1971): Wakefieldite, yttrium vanadate: a new mineral from Quebec. *Am. Mineral.*, **56**, 395-410.

Moriyami, T., Miyawaki, R., Yokoyama, K., Matsubara, S., Hirano, H., Murukami, H., Watanabe, Y. (2010): Wakefieldite-(Nd), a new neodymium vanadate mineral in the Arase stratiform ferromanganese deposit, Kochi Prefecture, Japan. *Res. Geol.*, **61**, 101-110.

Sallam, O.R., Alshami, A.S., Azab, M.S., El Akeed, I.A. (2014): The occurrence of silver-gold mineralization associated with uranium bearing minerals and base metal sulphide, El Sheik Soliman area, south Sinai, Egypt. *Egyptian J. Pure Appl. Sci.*, **52**, 47-54.

Stoppa, F., Pirajno, F., Schiazza, M. & Vladykin, N.V. (2016): State of the art: Italian carbonatites and their potential for critical-metal deposits. *Gondwana Res.*, **37**, 152-

171.

Van Panhuys-Sigler, M., Trewin, N.H., Still, J. (2018): Roscoelite associated with reduction spots in Devonian red beds, Gamrie Bay, Banffshire. *Scot. J. Geol.*, **32**, 127-132.

Witzke, T., Kolitsch, U., Warnsloh, J.M., Göske, J. (2008): Wakefieldite-(La), $LaVO_4$, a new mineral species from the Glűcksstern Mine, Friedrichroda, Thuringia, Germany. *Eur. J. Mineral.*, **20**, 1135-1139.